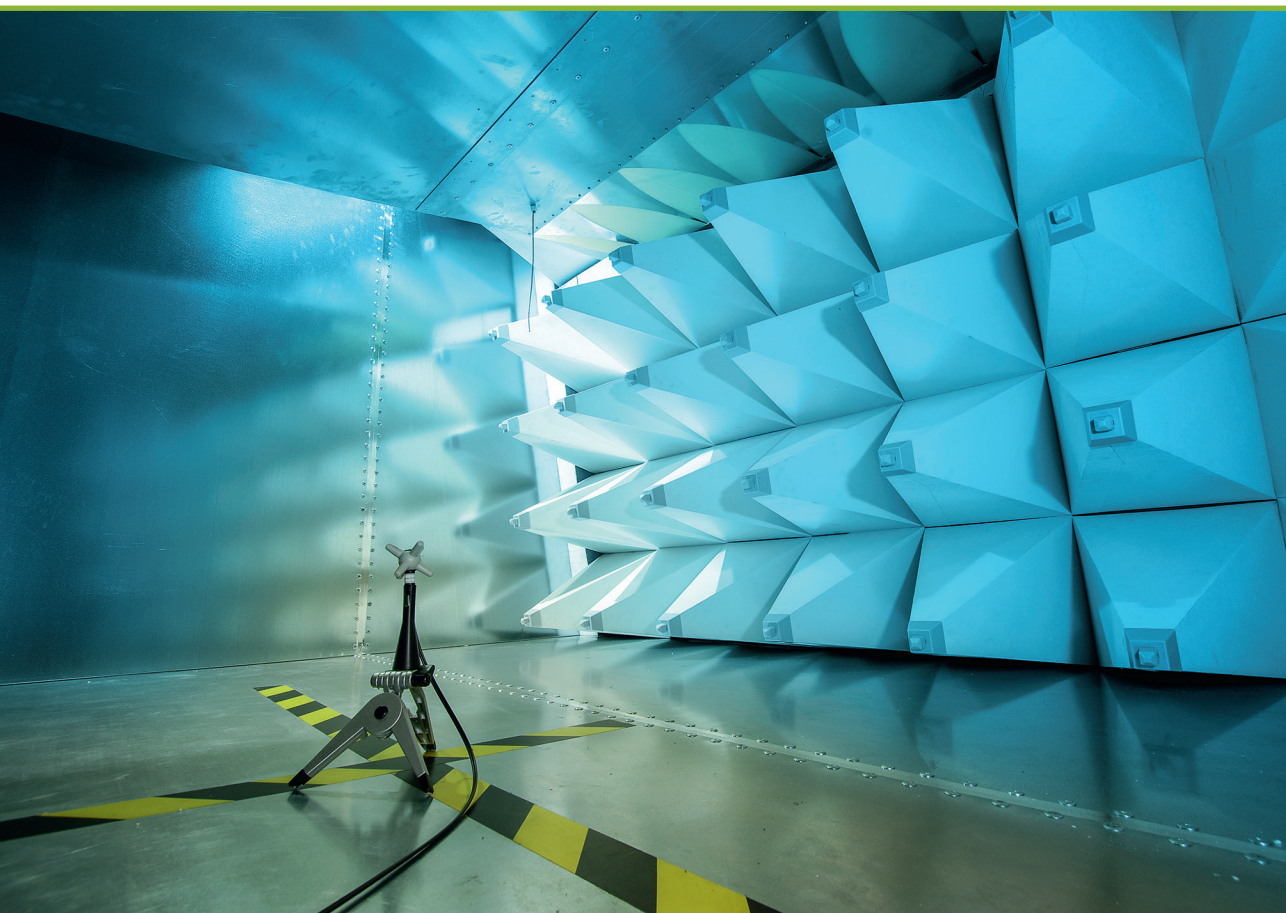


**Romāns Kušņins**

**MODEL SENSITIVITY EVALUATION AND  
DIELECTRIC CONSTANT MEASUREMENT  
UNCERTAINTY REDUCTION**

Summary of the Doctoral Thesis



**RIGA TECHNICAL UNIVERSITY**

Faculty of Electronics and Telecommunications

Institute of Radioelectronics

**Romāns Kušņins**

Student of the doctoral study program “Electronics”

**MODEL SENSITIVITY EVALUATION AND  
DIELECTRIC CONSTANT  
MEASUREMENT UNCERTAINTY  
REDUCTION**

**Summary of the Doctoral Thesis**

Scientific supervisor:  
Assistant Professor Dr. sc. ing.  
**JĀNIS SEMEŅAKO**

RTU Press  
Riga 2023

Kušņins, R. Model Sensitivity Evaluation and Dielectric Constant Measurement Uncertainty Reduction. Summary of the Doctoral Thesis. Riga: RTU Press, 2023. 47 p.

Published in accordance with the decision of the Promotion Council “RTU P-08” of 26 January 2023, Minutes No. 18.

NATIONAL  
DEVELOPMENT  
PLAN 2020



EUROPEAN UNION  
European Social  
Fund

---

INVESTING IN YOUR FUTURE

This work has been supported by the European Social Fund within the Project No. 8.2.2.0/20/I/008 “Strengthening of PhD students and academic personnel of Riga Technical University and BA School of Business and Finance in the strategic fields of specialization” of the Specific Objective 8.2.2 “To Strengthen Academic Staff of Higher Education Institutions in Strategic Specialization Areas” of the Operational Programme “Growth and Employment”

<https://doi.org/10.7250/9789934228896>

ISBN 978-9934-22-889-6 (pdf)

**DOCTORAL THESIS PROPOSED TO RIGA TECHNICAL  
UNIVERSITY FOR THE PROMOTION TO THE SCIENTIFIC  
DEGREE OF DOCTOR OF SCIENCE**

To be granted the scientific degree of Doctor of Science (Ph. D.), the present Doctoral Thesis has been submitted for the defence at the open meeting of RTU Promotion Council on 31 March 2023 at 11 a.m. at the Faculty of Electronics and Telecommunications of Riga Technical University, 12 Azenes Street, Room 201.

OFFICIAL REVIEWERS

Professor Dr. sc. ing. Dmitrijs Pikuļins  
Riga Technical University

Professor Dr.-Ing. Ingo Gaspard  
Hochschule Darmstadt, University of Applied Sciences, Germany

Associate Professor Dr. Darius Plonis  
Vilnius Gediminas Technical University, Lithuania

DECLARATION OF ACADEMIC INTEGRITY

I hereby declare that the Doctoral Thesis submitted for the review to Riga Technical University for the promotion to the scientific degree of Doctor of Science (Ph. D.) is my own. I confirm that this Doctoral Thesis had not been submitted to any other university for the promotion to a scientific degree.

Romāns Kušņins .....

Date: .....

The Doctoral Thesis has been written in English. It consists of an Introduction, 6 chapters, Conclusions, 54 figures, 13 tables; the total number of pages is 128. The Bibliography contains 138 titles.

## CONTENTS

|   |    |
|---|----|
| ABBREVIATIONS.....  | 5  |
| GENERAL OVERVIEW OF THE THESIS .....                                      | 6  |
| Rationale.....  | 6  |
| Aim of the Thesis and Defended Theses.....                                | 8  |
| Main Tasks .....  | 9  |
| Research Methods .....  | 9  |
| Scientific Novelty.....   | 10 |
| Main Results of the Thesis.....   | 10 |
| Publications and Approbation of the Thesis .....                          | 11 |
| 1 STRUCTURE OF THE THESIS AND RESULTS OBTAINED.....                       | 14 |
| 2 THESIS CHAPTER SUMMARIES .....  | 16 |
| 2.1 Measurement Uncertainty Estimation and Model Evaluation .....         | 16 |
| 2.2 Conventional Dielectric Constant Measurement Models.....              | 17 |
| 2.3 Extended Multi-slab Measurement Models for the Waveguide Method ..... | 24 |
| 2.4 Extended Multi-slab Measurement Models for the Free Space Method..... | 32 |
| 2.5 Extended Two-Rod Measurement Model for the Waveguide Method.....      | 36 |
| 2.6 Fast Integral Equation Method.....                                    | 38 |
| CONCLUSIONS .....   | 43 |
| BIBLIOGRAPHY.....   | 45 |

## ABBREVIATIONS

|            |   |
|------------|---|
| <b>EPM</b> | Error Propagation Method                              |
| <b>GUM</b> | Guide to the Expression of Uncertainty in Measurement |
| <b>FEM</b> | Finite Element Method                                 |
| <b>MCM</b> | Monte Carlo method                                    |
| <b>MoM</b> | Method of Moments                                     |
| <b>MUT</b> | Material Under Test                                   |
| <b>VNA</b> | Vector Network Analyzer                               |

# GENERAL OVERVIEW OF THE THESIS

## Rationale

Accurate measurements of dielectric constant are essential in many fields, including, among others, microwave technology, biology, agriculture, medicine, etc. [1]–[3]. However, there are many factors that significantly limit the accuracy of measurements, the most common of which are the limited resolution of measurement devices, systematic uncertainty, non-ideal alignment, reflection at junctions, slight shifts in the sample position in the model from the required, etc. [4], [5] While for some specialized microwave devices, e.g., in filters, the effect of the uncertainty of dielectric constant measurements on the performance can be partially compensated by employing additional tuning elements that, however, increases the cost of the final product, in other areas, e.g., in medicine, it is much more difficult and more expensive to achieve, and in some cases even impossible at all.

There are a variety of dielectric constant measurement methods [6], [7], the most commonly used being the resonant cavity method, the transmission-line method, and the free space method; however, each of these methods has a number of advantages and disadvantages. For example, the resonant cavity method provides high accuracy of the dielectric constant and loss tangent measurements for low-loss materials [8], but, unfortunately, requires quite expensive equipment and involves a very cumbersome and lengthy sample preparation process. The main drawback of this method is the fact that it is complicated to perform measurements at different frequencies [9], since the frequency in this measurement model is a quantity that is being measured directly. Therefore, the method is not suitable for measuring dielectrics with pronounced dispersion when both dielectric constant and loss tangent vary rapidly with frequency. Furthermore, the resonant techniques in the vast majority of cases require destructing the sample.

Although non-resonant measurement methods typically provide accuracy lower than that of their resonant counterparts, they, however, are less expensive and, in most cases, are non-destructive, which might be of particular importance in many applications [10], [11].

In the Thesis, an extensively used reflection-only method (only the scattering matrix element  $S_{11}$  is measured) is investigated, which is convenient and ensures reasonable measurement accuracy. It is demonstrated that in the case of the reflection-only (as well as reflection/transmission) measurements, especially when the measurements have to be non-destructive, the low model sensitivity problem may arise (the same applies to other measurement methods). Specifically, for certain dimensions of the sample under test, frequencies, dielectric constant values, or certain value ranges, the measurement uncertainty may be so large that the results of such measurements would be absolutely useless from the practical point of view. It is shown that a considerable measurement uncertainty results from a low sensitivity of the measurement model, which shows how sensitive is the measured absolute value of  $S_{11}$  to small variations in the dielectric constant value.

In this research, the measurement procedure and the mathematical relations between the measured quantity (dielectric constant) and the other quantities on which it depends is a mea-

surement model. A measurement model containing only a sample made of the material under investigation (MUT), the material whose dielectric constant is to be determined, is referred to throughout the Thesis as a conventional measurement model.

The Thesis demonstrates that the measurement model sensitivity plays a crucial role, as it immediately shows whether a specific measurement model is suitable for the measurements or not for a particular set of model parameter values (dielectric constant, sample dimensions, frequency). Also, it is shown that increasing the model sensitivity results in a reduction in the dielectric constant measurement uncertainty. A conventional measurement model is considered suitable for measurements if it exhibits a sufficiently high measurement model sensitivity; otherwise, one should consider using another measurement model that provides a higher sensitivity.

The Thesis also shows that the sensitivity of the measurement model can be improved by changing the sample dimensions and/or frequency; however, such an approach is not always feasible and permissible and may even be technologically unrealizable. For example, the frequency cannot be changed when the dielectric constant of the material under test has to be measured at a fixed standard defined frequency. At the same time, the dimensions cannot be altered when a ready-made product needs to be tested, such as cylindrical dielectric resonators extensively employed in resonant cavity-based microwave filters.

In this work, cylindrical samples (rods) and dielectric slabs are investigated.

A simple measurement model evaluation methodology is proposed and studied. The methodology allows for a quick and easy evaluation of the measurement model sensitivity for a conventional model. If the conventional model is found not to provide a sufficient sensitivity level, it allows for constructing an extended measurement model with such parameter values that for the expected dielectric constant value range, its sensitivity is higher than that of the conventional model, thereby significantly reducing the dielectric constant measurement uncertainty.

In the Thesis, the two most commonly used methods are used for estimating measurement uncertainty, which is recommended and recognized by GUM – the uncertainty propagation method [12], [13] and the Monte Carlo (MC) method [14]. The most commonly used in practice is the Error Propagation Method (EPM), which is well suited for models not exhibiting pronounced nonlinearity, as it is based on a Taylor series-based linear approximation about the point corresponding to the mean value of the measurand (best estimate). Furthermore, all input variables are assumed to be random quantities following a normal distribution. Despite the fact that such an approximation gives acceptable results in many practical cases, it can provide inaccurate results for models that have a very pronounced nonlinearity in the neighborhood of the actual value of the measurand, and when it is necessary to estimate the measurement uncertainty in the range of values of the measurement model parameters, where the dependence of the measurand on the model parameters is non-linear, the use of the EPM method may result in a significant overestimation or underestimation of the uncertainty [15].

The evaluation can also be done with the MC method [16], which can also be applied to models with pronounced nonlinearity, but it requires a large amount of computing and is also not always applicable. Despite the fact that the Monte Carlo method is applicable to a

much broader class of measurement models compared to EPM, it is unfortunately very time-consuming, mainly because it is necessary to calculate the output of the measurement model for a huge number of random combinations of the values of the model inputs, which is needed, to obtain a reliable estimate of the measurand. The Monte Carlo method is extensively used in many fields, such as metrology, optics, electronics, electromagnetic compatibility, etc. [17]. The GUM defines this method as the primary method for measurement uncertainty estimation.

However, the MC method requires solving the inverse problem for each model parameter value combination to estimate the uncertainty. Namely, at each iteration of the MC algorithm, the dielectric constant value corresponding to the measured value of the scattering matrix element must be determined, requiring a large number of arithmetic operations, thereby making the estimation impractical unless high-power computation resources are leveraged. Therefore, accurately estimating the uncertainty in the measurement of material constitutive properties is still challenging.

Numerical studies were performed to verify the effectiveness of the proposed methodology. The results successfully confirm the hypothesis that the reduction of measurement uncertainty for the problematic ranges of dielectric constant values, where the sensitivity is very low, can be achieved with the use of slightly more complex measurement models involving one or two auxiliary dielectric objects (rods or slabs, depending on the model type).

### **Aim of the Thesis and Defended Theses**

In order to address the problems mentioned above related to the effective evaluation of the suitability of dielectric constant measurement models, the selection of models, and the development of measurement models that ensure sufficiently small measurement uncertainty, the following main objectives of the work are put forward:

- develop a methodology for simple evaluation of the measurement model sensitivity;
- develop improved measurement models ensuring a sufficiently high model sensitivity in cases where conventional measurement models cannot accomplish it.

In order to achieve the main objectives of the Thesis, the following theses were defined:

1. The sensitivity of the measurement model depends on the selected measurement method, and for a sample with a specific shape and dimensions at a specific measurement frequency, the sensitivity strongly depends on the expected value of the dielectric constant and takes values in the range from 0 to 20.
2. The sensitivity of the measurement model is related to the measurement uncertainty, and if the model sensitivity is less than 1, then the relative uncertainty of the dielectric constant measurement is greater than 1 %.
3. To evaluate the suitability of the measurement model, it is not necessary to solve the time-consuming inverse problems for the measurement uncertainty estimation, as it suffices to

evaluate the sensitivity of the model from a solution to the forward problem using the Error Propagation Method, which reduces the model evaluation time, at least an order of magnitude.

4. If the conventional measurement model has a measurement sensitivity of less than 1, such a model is considered not suitable for the dielectric constant measurements, and an extended measurement model must be constructed by adding a dielectric slab or rod, the dimensions, position, and dielectric constant of which are calculated in such a way as to ensure the sensitivity of the measurement model greater than 1.
5. To be able to perform the dielectric constant measurement uncertainty estimation for models involving dielectric rods, it is necessary to develop a fast numerical method that is at least 50 times faster than currently existing methods.

### **Main Tasks**

1. To show that one can quickly and easily evaluate the sensitivity of the measurement model for any specific set of model parameter values to determine whether the model is suitable for the measurement or whether the measurement uncertainty will be unacceptably high. Additionally, the evaluation procedure allows for determining whether the model can ensure a specific measurement uncertainty.
2. To prove that the dielectric constant measurement uncertainty is closely related to the measurement model sensitivity and, therefore, the uncertainty can be reduced by increasing the model sensitivity.
3. To show that it is possible to increase the sensitivity of the measurement model for a specific set of model parameters by extending a conventional measurement model, which is accomplished by placing an additional object (or objects) or by altering the dimensions of the MUT or the frequency, provided that such alterations are permitted.
4. To develop a methodology and computer programs for constructing optimal extended models for specific cases.
5. To develop a numerical method for the calculation of the scattering matrix elements for dielectric constant measurement models involving dielectric rods in a rectangular waveguide, which provides at least 50 times faster measurement uncertainty estimation than currently existing methods.

### **Research Methods**

During the development of the Thesis, analytical and numerical calculations, as well as computer modeling are employed to achieve the objectives of the Thesis and perform problem analysis.

For calculating the scattering parameters of the dielectric constant measurement model with dielectric rods in a rectangular waveguide, the fast calculation method developed by the author, namely, the method of surface integral equations, is used.

Commercially available software Ansys HFSS is also used in the Thesis, mainly to check the accuracy and efficiency of the Improved Boundary Integral Equation Method developed by the author. The inverse problems are solved by means of the Newton-Rafson method.

Computer programs implemented in Python and C++ programming languages were developed to calculate the scattering parameters of the measurement models studied in the Thesis and evaluate the dielectric constant measurement uncertainty.

The programs intended for solving time-consuming tasks, for example, the calculation of Schlömilch series using the Ewald method, were implemented in C++ language, and the parallel data processing libraries OpenMP and OpenMPI are used to speed up the calculations.

The other programs were implemented in the Python programming language, including program packages for drawing graphs developed by the author.

### **Scientific Novelty**

- A simple Error Propagation Method based methodology for evaluating the sensitivity of a measurement for quick evaluation of the suitability of a specific measurement model for achieving a certain measurement uncertainty in dielectric constant measurements without extensive computing under non-destructing fixed frequency measurement scenario when the MUT in the measurement model is a slab or a rod in a waveguide or a dielectric slab in free space.
- A new two-slab waveguide or free-space measurement model to reduce the uncertainty in the dielectric constant measurements via increasing the measurement model sensitivity.
- A new three-slab waveguide or free space measurement model to reduce the dielectric constant measurement uncertainty via increasing the measurement model sensitivity.
- A new measurement model, composed of two dielectric rods in a rectangular waveguide, reducing the dielectric constant measurement uncertainty by increasing the measurement model sensitivity.
- A new efficient numerical method for calculating the dominant waveguide mode scattering matrix elements for multi-layered full-height rods in a rectangular waveguide. The rods can have an arbitrary number of dielectric inclusions.

### **Main Results of the Thesis**

1. The developed measurement model sensitivity evaluation methodology for determining whether the range of possible dielectric constant values is in a measurement model low-

sensitivity range, giving measurement uncertainty too large to ensure acceptable measurement accuracy under a non-destructive fixed frequency waveguide or free space measurement scenario.

2. The use of the extended dielectric constant measurement models, in some instances, provides model sensitivity that is significantly higher than that of the conventional model, which contains only the object under test (rod or slab), resulting in smaller measurement uncertainty. The measurement models investigated in the Thesis are:
  - a dielectric slab, the constant of which is determined from the measured value of the modulus of the scattering matrix element  $S_{11}$  measured for the dominant rectangular waveguide mode (in the case of waveguide measurements) or a plane wave (in the case of the free-space measurement model) and extended models with two or three dielectric slabs, one of which is a slab of material to be measured;
  - a dielectric rod in a rectangular waveguide with a dielectric constant to be determined from the measured absolute value of the scattering matrix element  $S_{11}$  for the dominant waveguide mode and extended models with an auxiliary dielectric rod of known constitutive properties and dimensions.
3. The developed numerical methods for solving integral equations, which use the Ewald method for the calculation of slowly converging Schlömilch series, allows for calculating scattering parameters for structures consisting of multiple full-height dielectric rods in a rectangular waveguide, up to 500 times faster than commercially available finite element method based software.

## **Publications and Approbation of the Thesis**

**The results of the Doctoral Thesis have been presented at 5 scientific conferences and workshops whose proceedings are indexed in SCOPUS, WoS, and IEEE databases.**

1. Kushnin, R., Semenjako, J. “Determination of the Optimal Value of the Radius of a Circular Cylindrical Post in a Rectangular Waveguide for Measurement of the Dielectric Permittivity”, presented at Progress in Electromagnetic Research Symposium (PIERS 2013), Sweden, Stockholm, 12–15 August 2013.
2. Kushnin, R., Semenjako, J., and Solovjova, T. “Determination of Optimal Pairs of Radii of Dielectric Samples for Complex Permittivity Measurement of Dispersive Materials”, presented Progress in Electromagnetics Research Symposium (PIERS2015), Czech Republic, Prague, 6–9 July 2015.
3. Kushnin, R., Semenjako, J., and Shestopalov, Y. V. “Accelerated Boundary Integral Method for Solving the Problem of Scattering by Multiple Multilayered Circular Cylindrical Posts in a Rectangular Waveguide”, presented at Progress in Electromagnetics Research Symposium - Spring (PIERS 2017), Russia, Saint Petersburg, 22–25 May 2017.

4. Kimsis, K., Semenjako, J., Kushnin, R., Viduzs, A. “Numerical Implementation of Efficient Cross-section Method for the Analysis of Arbitrarily Shaped Dielectric Obstacles in Rectangular Waveguide”, presented at Progress in Electromagnetics Research Symposium – Spring (PIERS 2017), Russia, Saint Petersburg, 22–25 May 2017.
5. Kushnin, R., Semenjako, J., and Shestopalov Y. V. “Fast Method for Analysis of Multiple H-Plane Cylindrical Posts with Multiple Cylindrical Inclusions in a Rectangular Waveguide”, presented at the 2020 IEEE Microwave Theory and Techniques in Wireless Communications (MTTW), Oct. 2020.

**The results of the Doctoral Thesis are presented in 9 out of 14 author’s scientific articles and in publications in conference proceeding indexed in SCOPUS, WoS, and IEEE databases.**

1. Kushnin, R., Semenjako, J. “Scattering by a Layered Circular Cylindrical Post in a Rectangular Waveguide”. Telecommunications and Electronics. Vol. 11, 2011, pp. 41–48. ISSN 1407-8880.
2. Kushnin, R., Semenjako, J. “Determination of the Optimal Value of the Radius of a Circular Cylindrical Post in a Rectangular Waveguide for Measurement of the Dielectric Permittivity”. In: Progress in Electromagnetic Research Symposium(PIERS 2013): Proceedings, Sweden, Stockholm, 12–15 August 2013. Stockholm: The Electromagnetics Academy, 2013, pp. 52–57.
3. Kushnin, R., Semenjako, J., Solovjova, T. “Determination of Optimal Pairs of Radii of Dielectric Samples for Complex Permittivity Measurement of Dispersive Materials”. In: Progress in Electromagnetics Research Symposium (PIERS2015): Proceedings, Czech Republic, Prague, 6–9 July 2015. Prague: The Electromagnetics Academy, 2015, pp. 2320–2325.
4. Kushnin, R., Semenjako, J., Shestopalov, Y. V. “Accelerated Boundary Integral Method for Solving the Problem of Scattering by Multiple Multilayered Circular Cylindrical Posts in a Rectangular Waveguide”. In: 2017 Progress in Electromagnetics Research Symposium – Spring (PIERS), Russia, St.Petersburg, 22–25 May 2017. Piscataway: IEEE, 2017, pp. 3263–3271.
5. Kimsis, K., Semenjako, J., Kushin, R., Vidužs, A. “Numerical Implementation of Efficient Cross-section Method for the Analysis of Arbitrarily Shaped Dielectric Obstacles in Rectangular Waveguide”. In: 2017 Progress in Electromagnetics Research Symposium – Spring (PIERS 2017): Proceedings, Russia, Saint Petersburg, 22–25 May 2017. Piscataway: IEEE, 2018, pp. 3937–3943.
6. Kushnin, R., Semenjako, J., Shestopalov, Y. V. “Maximum-Sensitivity Method for Minimizing Uncertainty in the Measurements of Permittivity of a Cylindrical Dielectric Sam-

ple in a Rectangular Waveguide”. In: 2017 Progress in Electromagnetics Research Symposium - Fall (PIERS - FALL): Proceedings, Singapore, Singapore, 19–22 November 2017. Piscataway: IEEE, 2018, pp. 570–578. ISBN 978-1-5386-1212-5. e-ISBN 978-1-5386-1211-8.

7. Kushins, R., Semenjako, J., Shestopalov, Y. V., Vidužs, A. “Two-slab High Sensitivity Technique for Measurement of Permittivity of a Dielectric Slab in a Rectangular Waveguide”. In: Progress in Electromagnetics Research Symposium 2018: Proceedings, Japan, Toyama, 1–4 August 2018. Piscataway: IEEE, 2018, pp. 176–183.
8. Kushin, R., Kuzminovs, G., Semenjako J., Shestopalov Y. V. “Novel High-sensitivity Non-destructive Technique for the Measurement of Permittivity of a Low-loss Dielectric Slab in Free Space”. 2019 Photonics & Electromagnetics Research Symposium – Spring (PIERS-Spring), 2019, pp. 1723–1731, doi: 10.1109/PIERS-Spring46901.2019.9017638.
9. Kushnin, R., Semenjako, J., Shestopalov Y. V. “Fast Method for Analysis of Multiple H-Plane Cylindrical Posts with Multiple Cylindrical Inclusions in a Rectangular Waveguide”. 2020 IEEE Microwave Theory and Techniques in Wireless Communications (MTTW), 2020, pp. 190–194, doi: 10.1109/MTTW51045.2020.9244922.

# 1. STRUCTURE OF THE THESIS AND RESULTS OBTAINED

The Thesis contains an introduction, six chapters, conclusions and bibliography.

The introduction of the Thesis describes the relevance and the main aims of the Thesis, as well as the tasks, research methodology, scientific novelty of the proposed methodologies, main results of the Thesis, approbation and publications.

Chapter 1 defines several terms used throughout the Thesis, such as the measurement model, measurement curve, discusses the measurement uncertainty methods used for obtaining the results presented in the Thesis, as well as their advantages and disadvantages, and introduces the measurement model sensitivity coefficient, which is essential in the evaluation of measurement models. Also, the methods of solving inverse problems and approaches to reducing the measurement uncertainty are discussed, and the importance of the tentative measurement model sensitivity evaluation, which is not adequately reflected and studied in the existing literature, is demonstrated in this chapter.

In Chapter 2, three conventional measurement models are described and examined, namely, a single dielectric slab in a waveguide and free space, as well as a cylindrical dielectric rod in a waveguide. In all models, low-loss dielectrics are measured, and the dielectric constant of the MUT is extracted from the measured value of  $|S_{11}|$  by solving the inverse problem. The dependence of the model behavior on the expected dielectric constant of the MUT is investigated, and the results of the numerical calculations demonstrate that the model sensitivity depends considerably on the set of input parameters (sample dimensions, frequency, and the dielectric constant of the MUT); thus, the essence of the research problem is described and clearly illustrated – measurement uncertainties depend significantly on the sensitivity of the chosen measurement model for a specific set of the model input parameters. It is demonstrated that for certain conventional measurement model parameter (sample dimensions, dielectric constant, and frequency) values, the measurement uncertainty may be so large that the measurement results become practically irrelevant and that the inadequacy of the model can be evaluated in a simple manner without having to solve the inverse problem.

Chapter 3 describes and illustrates a novel and effective methodology proposed by the author of the Thesis for reducing the low-loss material dielectric constant measurement uncertainty. The proposed expanded dielectric constant measurement model is described and examined. The model may involve a MUT slab along with an additional slab placed at a certain distance from the MUT slab or the MUT slab alongside two additional slabs. In contrast to the conventional measurement model, which involves the MUT only, a dielectric slab in the waveguide made of the material to be measured, the extended model incorporates one or two more dielectric slabs, whose thickness and dielectric constant are determined such that the sensitivity of the measurement model is increased. The extended measurement models, which increase the sensitivity of the conventional model, make it possible to reduce the measurement uncertainty without changing the experimental conditions (MUT dimensions, frequency, measurement model).

Chapter 4 describes the extended dielectric constant measurement model with the free space

method. Similar to the conventional waveguide model, the free space model involves not only the MUT, which is a dielectric slab, but also one or two auxiliary slabs also located in free space parallel to the MUT slab. Two extended models are proposed, analyzed and optimized: a two-slab model and a three-slab model. It is shown that in case the conventional model is not capable of providing a sufficiently high measurement model sensitivity, it is possible to increase the sensitivity by extending the model, thus ensuring a lower measurement uncertainty compared to the conventional model.

Chapter 5 describes the extended two-rod dielectric constant measurement model for the waveguide method. This model consists of two dielectric cylindrical rods in a rectangular waveguide. One of the rods is made of MUT whose dielectric constant is to be determined from the measured value. The second rod is an auxiliary rod whose location, radius and dielectric constant are chosen so that the extended model ensures the highest possible model sensitivity. The measurements are performed in single-mode regime at a single frequency (often chosen to meet standard requirements). It is shown that in cases where the conventional model involving the MUT rod only fails to provide sufficient model sensitivity, it can be increased by using the extended measurement model.

Chapter 6 describes the method developed by the author for the calculation of scattering parameters for structures composed of one or more multi-layered cylindrical rods in a rectangular waveguide. Each rod can be either centered or offset and may be either dielectric or metallic.

The method is, in essence, a surface integral equations method in which the unknown functions to be found are the electric and magnetic fields on the surfaces of the cylindrical rods. The integration required for the evaluation of the entries of the resulting system of algebraic equations is performed analytically, which gives slowly converging Schlömilch series. The convergence of the series is accelerated by means of the Ewald summation technique, thereby significantly reducing the calculation time, which is much less compared to similar methods.

Discussion of the obtained analytical and numerical results, result comparison, and model evaluation concludes the Thesis. Also, it is concluded that the tasks defined in the Thesis have been successfully accomplished and the theses have been proven.

## 2. THESIS CHAPTER SUMMARIES

### 2.1. Measurement Uncertainty Estimation and Model Evaluation

Chapter 1 of the Thesis describes the measurement uncertainty estimation using the Error Propagation Method (EPM) and the Monte Carlo Method (MCM). Additionally, methods for solving inverse problems are briefly described.

The dielectric constant of the measured material is determined from the measured magnitude of the scattering matrix element  $S_{11}$  by solving the inverse problem. In the Thesis, the inverse problem is solved using the Newton-Raphson method. It is assumed that the expected value of the dielectric constant of a sample made of the material under test (MUT) is approximately known, and the MUT has low losses, which are assumed to be measured beforehand by another method or provided by the manufacturer. This approach is widely used in high-frequency dielectric testing, which is made in such a way that their losses are as small as possible.

To estimate the uncertainty of the MUT dielectric constant measurements, the EPM, which is one of the most commonly used methods, as well as the extended error propagation method, can be employed [12]. In the EPM, the uncertainty is calculated as follows:

$$u(\varepsilon'_{r,\text{mut}}) = \sqrt{u_{|S_{11}|}^2(\varepsilon'_{r,\text{mut}}) + u_{d_{\text{mut}}}^2(\varepsilon'_{r,\text{mut}}) + u_f^2(\varepsilon'_{r,\text{mut}}) + u_{\tan\delta_{\text{mut}}}^2(\varepsilon'_{r,\text{mut}})}. \quad (2.1)$$

Slightly rearranging (2.1) gives the following expression that is more illustrative from the point of view of the main objective of the Thesis. Namely, it shows that the factor  $\frac{\partial |S_{11}|}{\partial \varepsilon'_{r,\text{mut}}}$  plays an essential role in the model evaluation in terms of the measurement accuracy, as discussed below.

$$u(\varepsilon'_{r,\text{mut}}) = \frac{1}{\frac{\partial |S_{11}|}{\partial \varepsilon'_{r,\text{mut}}}} \cdot \sqrt{(u_{|S_{11}|})^2 + \left(\frac{\partial |S_{11}|}{\partial d_{\text{mut}}} u_{d_{\text{mut}}}\right)^2 + \left(\frac{\partial |S_{11}|}{\partial f} u_f\right)^2 + \left(\frac{\partial |S_{11}|}{\partial \tan \delta_{\text{mut}}} u_{\tan \delta_{\text{mut}}}\right)^2}. \quad (2.2)$$

The quantities appearing in the radicand are the contributions of individual parameters of the measurement model to the total uncertainty of dielectric constant measurements and are given by:

$$u_{|S_{11}|}(\varepsilon'_{r,\text{mut}}) = \frac{\partial \varepsilon'_{r,\text{mut}}}{\partial |S_{11}|} u_{|S_{11}|} - \text{the measurement uncertainty contribution of } |S_{11}|;$$

$$u_{d_{\text{mut}}}(\varepsilon'_{r,\text{mut}}) = \frac{\partial \varepsilon'_{r,\text{mut}}}{\partial d_{\text{mut}}} u_{d_{\text{mut}}} - \text{the MUT slab thickness measurement uncertainty contribution;}$$

$$u_f(\varepsilon'_{r,\text{mut}}) = \frac{\partial \varepsilon'_{r,\text{mut}}}{\partial f} u_f - \text{the frequency measurement uncertainty contribution;}$$

$$u_a(\varepsilon'_{r,\text{mut}}) = \frac{\partial \varepsilon'_{r,\text{mut}}}{\partial a} u_a - \text{the waveguide width measurement uncertainty contribution;}$$

$$u_{\tan \delta_{\text{mut}}}(\varepsilon'_{r,\text{mut}}) = \frac{\partial \varepsilon'_{r,\text{mut}}}{\partial \tan \delta_{\text{mut}}} u_{\tan \delta_{\text{mut}}} - \text{the contribution of the MUT loss tangent measurement}$$

uncertainty,

where

- $u_{|S_{11}|}$  – the standard uncertainty of  $|S_{11}|$ ;
- $u_{d_{\text{mut}}}$  – the standard uncertainty of the MUT slab thickness, mm;
- $u_f$  – the standard uncertainty of the frequency, GHz;
- $u_a$  – the standard uncertainty of the waveguide width, mm;
- $u_{\tan \delta_{\text{mut}}}$  – the standard uncertainty of the MUT loss tangent.

In the case of models containing additional dielectric slabs or cylindrical rods alongside the MUT slabs (rod), the EPM expression for the measurement uncertainty calculation may contain additional terms of the form:

$$u_{\text{par},i}(\varepsilon'_{r,\text{mut}}) = \frac{\partial \varepsilon'}{\partial (\text{par},i)} u_{\text{par},i}, \quad (2.3)$$

where

- $u_{\text{par}}(\varepsilon'_{r,\text{mut}})$  – the contribution to measurement uncertainty of the  $i$ -th model input parameter;
- $u_{\text{par},i}$  – the standard uncertainty of the  $i$ -th model input parameter.

Additional model input parameters are, for example, the dielectric constant and the loss tangent of an additional slab in an extended measurement model formed from a conventional one containing the MUT only by placing an additional slab in the waveguide at a specific distance from the MUT slab. The distance between the additional and the MUT slabs may be treated as an additional model input parameter.

The first chapter of the Thesis also describes the application of the Monte Carlo method employed in this Thesis for measurement uncertainty estimation.

## 2.2. Conventional Dielectric Constant Measurement Models

Chapter 2 of the Thesis discusses conventional measurement models involving only a sample of the material to be measured (MUT).

Subsection 2.1.1 discusses a conventional model composed of a rectangular dielectric sample (slab) located in a rectangular waveguide. The slab is made of a material whose dielectric constant is to be measured (see Fig. 2.1). It is assumed that the dielectric slab is homogeneous and the waveguide walls are perfectly conducting. These assumptions appreciably simplify the mathematical model of the measurement model – it is possible to obtain simple analytical expressions for the calculation of  $S_{11}$  while not causing any significant discrepancies with experimental results. The waveguide is assumed to be a standard rectangular waveguide WR-90 with a width equal to 22.86 mm, and measurements are made at 10 GHz.

Throughout the Thesis, the curve  $|S_{11}(\varepsilon'_{r,\text{mut}})|$  (and similarly for other models) is termed the **model measurement curve**. As follows from Formula (2.2), the steepness of this curve, which is characterized by the derivative of  $|S_{11}|$  with respect to  $\varepsilon'_{r,\text{mut}}$ ,  $\frac{\partial |S_{11}|}{\partial \varepsilon'_{r,\text{mut}}} = \left( \frac{\partial \varepsilon'_{r,\text{mut}}}{\partial |S_{11}|} \right)^{-1}$ ,

is what ultimately determines how large the total measurement uncertainty will be, since the contribution of each model parameter is inversely proportional to the value of this quantity.

In the Thesis, the derivative  $\varepsilon_{r,\text{mut}}, \frac{\partial |S_{11}|}{\partial \varepsilon_{r,\text{mut}}}$  is referred to as the **measurement model sensitivity coefficient**. This coefficient clearly shows that in the value ranges where the measurement curve is almost parallel to the argument axis (the steepness of the curve is very low), it is actually impossible to measure the dielectric constant with this model, as the measurement uncertainty will be very large.

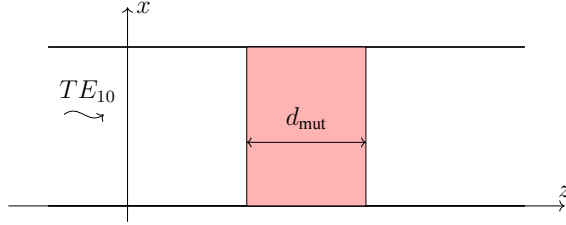


Fig. 2.1. The conventional single slabs waveguide measurement model.

The following expressions are for the scattering matrix entries of the model involving a single dielectric slab in a rectangular waveguide (or transmission line):

$$S_{11} = \frac{R_{\text{mut}}(1 - T_{\text{mut}}^2)}{1 - R_{\text{mut}}^2 T_{\text{mut}}^2} \quad (2.4)$$

where

$T_{\text{mut}} = e^{-j\tilde{k}d_{\text{mut}}}$  – the transmission coefficient;

$R_{\text{mut}} = (\tilde{k}_0 - \tilde{k})/(\tilde{k}_0 + \tilde{k})$  – the interfacial reflection coefficient at slab faces;

$\tilde{k}_0 = \sqrt{k_0^2 - (\pi/a)^2}$  – the  $TE_{10}$  mode waveguide wavenumber in the air-filled region, 1/m;

$\tilde{k} = \sqrt{k_0^2 \varepsilon_{r,\text{mut}} - (\pi/a)^2}$  – the  $TE_{10}$  mode waveguide wavenumber in the dielectric-filled region, 1/m;

$k_0 = 2\pi f/c$  – the free space wavenumber, 1/m;

$\varepsilon_{r,\text{mut}} = \varepsilon'_{r,\text{mut}} (1 - j \tan \delta_{\text{mut}})$  – the complex dielectric constant in the dielectric-filled region.

Figure 2.2 shows the calculated  $|S_{11}|$  plotted against the dielectric constant of the MUT sample,  $\varepsilon'_{r,\text{mut}}$  – a flat-faced slab filling the entire waveguide cross-section. In the figure, the dielectric constant measurement uncertainty is indicated by  $\Delta \varepsilon'_{r,\text{mut}}$ .

In Fig. 2.2 the widths of the red and blue horizontal bars are equal to the widths of the confidence interval of  $|S_{11}|$  values, which are chosen to be  $\Delta |S_{11}| = 0.01$ .

The width of the red vertical bar is equal to the confidence interval of the measured MUT sample dielectric constant when its actual value and the loss tangent value are equal to  $\varepsilon'_{r,\text{mut}} = 4.3$  and  $\tan \delta_{\text{mut}} = 0.003$ , respectively.

The width of the blue vertical bar is equal to the confidence interval width for the measured value dielectric constant in the case when the actual value of the MUT dielectric constant and the

MUT loss tangent are assumed to be equal to  $\varepsilon'_{r,\text{mut}} = 10.2$  and  $\tan \delta_{\text{mut}} = 0.0023$ , respectively.

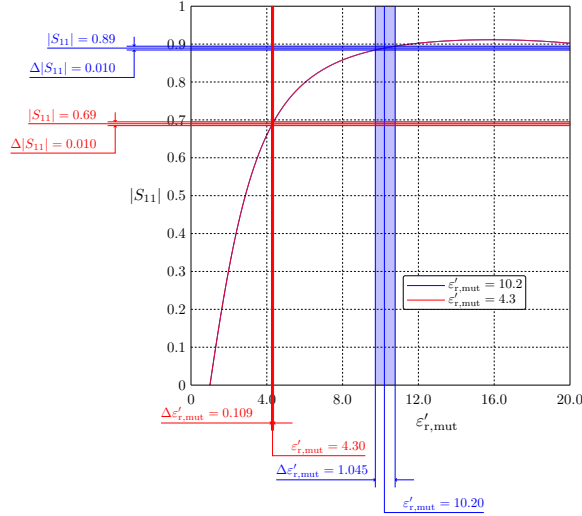


Fig. 2.2.  $|S_{11}|$  as a function of  $\varepsilon'_{r,\text{mut}}$  and the confidence intervals calculated for the model involving a single slab in a rectangular waveguide at different  $\varepsilon'_{r,\text{mut}}$  values.

As can be seen in Fig. 2.2, the uncertainty of the dielectric constant measurements depends on the expected (actual) value of the dielectric constant, and it may differ by an order of magnitude.

In addition, its value depends on the steepness of the measurement curve – for values of  $\varepsilon'_{r,\text{mut}}$  giving high steepness of the measurement curve, the measurement uncertainty is greater than for those which provide low curve steepness. This means that the suitability of the conventional measurement model can be deduced just by visually inspecting the plot of the measurement curve derivative  $\frac{\partial |S_{11}|}{\partial \varepsilon'_{r,\text{mut}}}$ .

Figure 2.3 shows  $|S_{11}|$  as a function of  $\varepsilon'_{r,\text{mut}}$  calculated for two samples of the same MUT with different thicknesses:  $d_{\text{mut}} = 2.5$  mm and  $d_{\text{mut}} = 0.635$  mm. The MUT is assumed to have the actual value of the dielectric constant equal to  $\varepsilon'_{r,\text{mut}} = 10.2$ , while the loss tangent value for the sample is  $\tan \delta_{\text{mut}} = 0.0023$ .

The curves of the calculated  $|S_{11}(\varepsilon'_{r,\text{mut}})|$  plotted in Fig. 2.3 show that there is a significant dependence of the dielectric constant measurement uncertainty on the thickness of the MUT slab. The calculation results show that for the slab with  $d_{\text{mut}} = 2.5$  mm, the width of the confidence interval for the dielectric constant values is more than four times larger than in the case of the slab thickness  $d_{\text{mut}} = 0.635$  mm. From this, it follows that the measurement uncertainty can be reduced by changing the thickness of the MUT sample; however, this may also result in increased uncertainty. Moreover, this approach to uncertainty reduction is not always permissible, e.g., when the finished product is to be measured, and it is challenging to process ceramic dielectrics without expensive precision machining equipment.

The results, as well as the expressions for the evaluation of  $|S_{11}|$ , show that  $|S_{11}|$  depends on  $d_{\text{mut}}/\lambda$ . It is assumed that the measurements are performed at a fixed frequency  $f = 10$  GHz, as required by many standards.

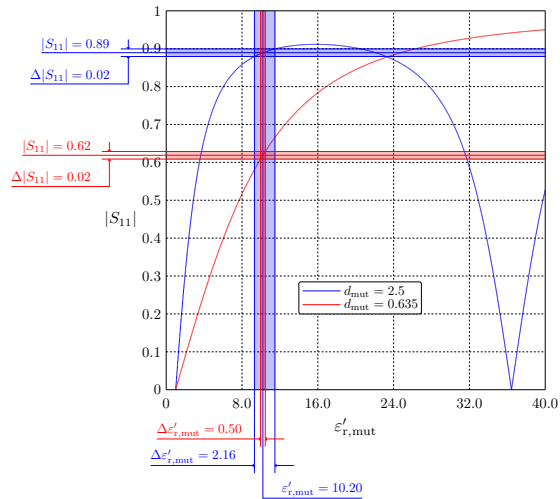


Fig. 2.3.  $|S_{11}|$  as a function of  $\epsilon'_{r,\text{mut}}$  and the confidence intervals at two different  $d_{r,\text{mut}}$ .

Subsection 2.1.2 discusses the conventional model consisting of a homogeneous MUT sample, which is geometrically a flat slab with infinite transverse dimensions and finite thickness located in free space. The slab is oriented so that its broader faces are perpendicular to the direction of the incident plane wave propagation; alternatively, it is assumed that the plane electromagnetic wave is incident normally on the slab. These assumptions greatly simplify the mathematical model of the measurement model - allow for obtaining compact analytical expressions for the calculation of  $|S_{11}|$ , giving results that do not cause any significant discrepancy with experimental results obtained for a slab with the same thickness, but finite transverse dimensions. The geometry of the model under study is illustrated in Fig. 2.4.

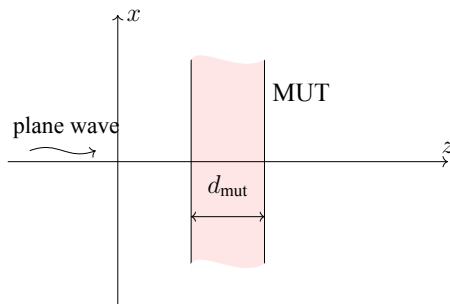


Fig. 2.4. The conventional single slab free space measurement model.

Figure 2.5 shows calculated  $|S_{11}|$  as a function of  $\varepsilon'_{r,\text{mut}}$  for two slabs with equal thicknesses  $d_{\text{mut}} = 2.0$  mm, but two different values of  $\varepsilon'_{r,\text{mut}}$  (see curves indicated in Fig. 2.3). Meanwhile, the curves plotted in Fig. 2.6 are obtained for the MUT, whose parameters are the same as those in Fig. 2.2, except for the thickness that is varied in this case.

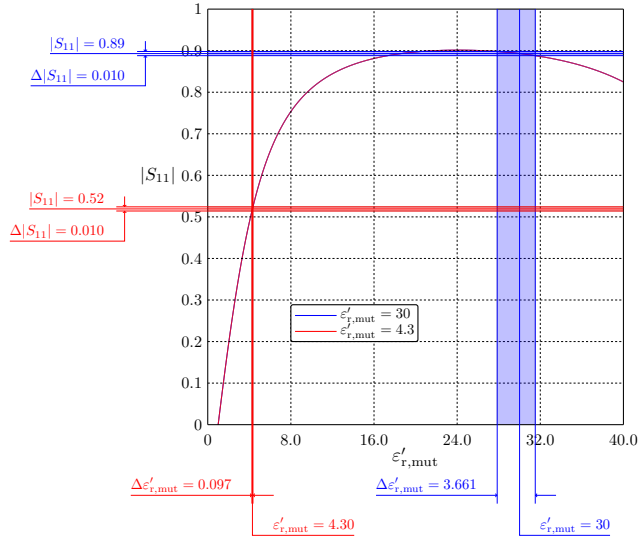


Fig. 2.5.  $|S_{11}|$  as a function of  $\varepsilon'_{r,\text{mut}}$  and the confidence intervals at two different  $\varepsilon'_{r,\text{mut}}$ .

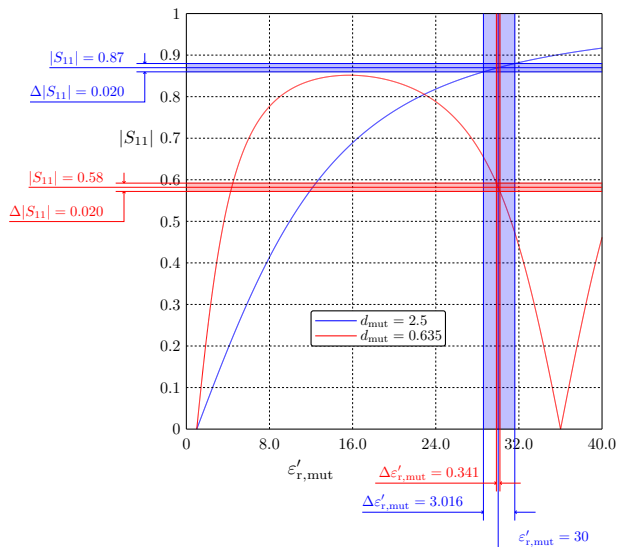


Fig. 2.6.  $|S_{11}|$  as a function of  $\varepsilon'_{r,\text{mut}}$  and the confidence intervals at two different  $d_{r,\text{mut}}$ .

The results are obtained for two MUT samples with different thicknesses equal to  $d_{\text{mut}} = 2.5 \text{ mm}$  and  $d_{\text{mut}} = 0.635 \text{ mm}$ , respectively. It is assumed that the measurement frequency is fixed at  $f = 10 \text{ GHz}$  and that the MUT dielectric constant and the MUT loss tangent is the same for both samples and are set equal to  $\epsilon'_{\text{r,mut}} = 30.0$  and  $\tan \delta_{\text{mut}} = 0.00067$ , respectively.

The results are similar to those of the conventional waveguide model – the measurement uncertainty is significantly affected by both  $\epsilon'_{\text{r,mut}}$ ,  $d_{\text{mut}}$  and frequency.

The expressions for the calculation of  $|S_{11}|$  for the free space waveguide measurement model differ slightly from those of the waveguide measurement model, and therefore, the results of the numerical calculations are different, which means that the results of the measurement models with the MUT slab in the waveguide and the MUT slab in the free space must be treated separately.

Subsection 2.2 discusses a conventional model comprising a dielectric cylindrical sample made of MUT placed in a rectangular waveguide. It is also assumed that the dielectric cylinder is homogeneous, its height is the same as that of the waveguide, its axis is parallel to the narrower waveguide wall, and the walls of the waveguide are perfectly electrically conducting. For this model, the quantity  $|S_{11}|$  is calculated using the Sahalos-Abdulnour mode-matching method adapted to structures composed of cylindrical dielectric full-height rods in a rectangular waveguide [18].

The geometry of the model under consideration is shown in Fig. 2.7.

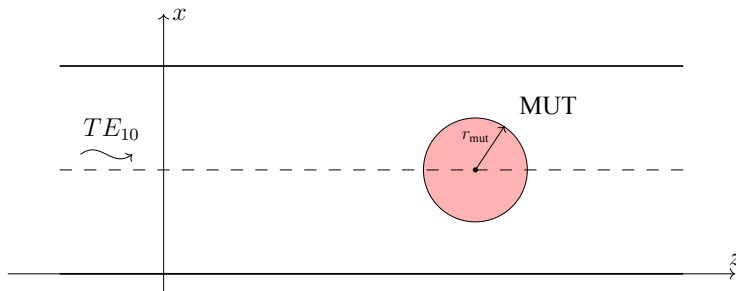


Fig. 2.7. The geometry of the conventional single rod waveguide measurement model.

The results are similar to those of the conventional waveguide model – the measurement uncertainty is significantly affected by  $\epsilon'_{\text{r,mut}}$ ,  $d_{\text{mut}}$  and also frequency. Figure 2.8 shows the calculated  $|S_{11}|$  as a function of  $\epsilon'_{\text{r,mut}}$ , as well as the measurement uncertainty calculated for two samples made of different dielectric materials with the same dielectric constant and loss tangent values as in the case of the model whose analysis results are presented in Fig. 2.2. Both cylindrical samples have the same radius  $r_{\text{mut}} = 2.5 \text{ mm}$

Additionally, the calculations for the two cylindrical samples of the same MUT with different radii show that, similar to the previous cases, the measurement uncertainty depends on the sample radius and frequency.

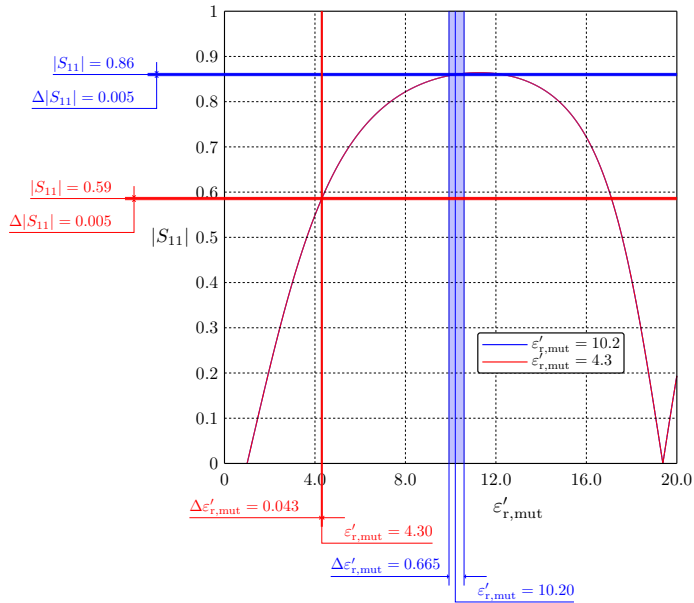


Fig. 2.8.  $|S_{11}|$  as a function of  $\epsilon'_{r,mut}$  and confidence intervals calculated for the model involving a cylindrical rod in a rectangular waveguide, at two different  $\epsilon'_{r,mut}$ .

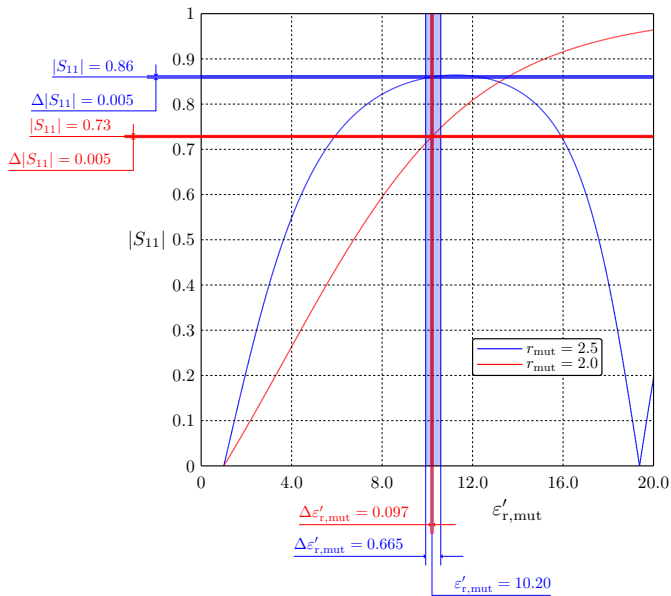


Fig. 2.9.  $|S_{11}|$  as a function of  $\epsilon'_{r,mut}$  and the confidence intervals at two different  $r_{mut}$ .

### 2.3. Extended Multi-slab Measurement Models for the Waveguide Method

In Chapter 3 of the Thesis, extended measurement models developed by the author are discussed. The models are composed of a dielectric slab with a dielectric constant to be measured (MUT slab) and one or two additional slabs employed to construct two-slab or three-slab measurement models.

Subsection 3.1. provides a brief overview of the use of extended measurement models and their optimization. Only a few such models have been proposed to date - mainly by E. J. Rothwell, and his students [2], [3]. Furthermore, there have been practically no studies on the construction of optimal models – models optimized in terms of sensitivity, in situations where conventional dielectric constant measurement models for a specific MUT sample do not ensure sufficiently high sensitivity. The conventional measurement slab model for the waveguide is a model comprising only a MUT slab made of the material whose dielectric constant is to be determined.

In Subsection 3.2, the measurement model proposed by the author is described and investigated. The model is composed of two slabs – the MUT slab and the second, additional slabs designed to increase the sensitivity of the measurement model. The two slabs are placed in a rectangular waveguide at a specific distance from each other. The faces of the slabs are parallel and oriented normally to the direction of the incident wave propagation. The measurement frequency is assumed to be fixed (as many standards require) and, in this case, is chosen to be 10 GHz. It is also assumed that the dielectric slabs are homogeneous and the waveguide walls are perfectly electrically conducting.

The waveguide is a standard rectangular waveguide WR-90 with an operating range of 8.20 to 12.40 GHz. This means that there is a single-mode regime in the waveguide – only the wave type  $TE_{10}$  propagates. The geometry of the model is depicted in Fig. 2.10. The above-mentioned assumptions significantly simplify the mathematical model of the measurement model – they allow for deriving compact closed-form expressions for the calculation of  $S_{11}$  while guaranteeing an acceptably small discrepancy between the actual results and the ones calculated with the aid of these expressions.

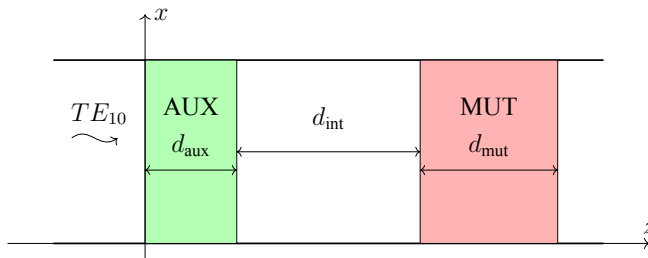


Fig. 2.10. The geometry of the two-slab waveguide measurement model.

If the interval of possible dielectric constant values coincides or overlaps with a low-sensitivity region of the conventional measurement model, the measurement uncertainty will be substantial. To mitigate this problem, one needs to alter the shape of the measurement curve

so that the sensitivity coefficient of the extended measurement model  $\frac{\partial |S_{11}|}{\partial \varepsilon'_{r,\text{mut}}}$  is sufficiently large in the interval of possible values of the measured quantity. The main idea of the proposed methodology is to achieve a significant reduction of measurement uncertainty by increasing the steepness of the curve, thereby increasing the measurement sensitivity,  $\frac{\partial |S_{11}|}{\partial \varepsilon'_{r,\text{mut}}}$ . Here  $\varepsilon'_{r,\text{mut}}$  denotes the relative dielectric constant of the material to be measured. In the calculations, it is assumed that performing measurements in the region where the value of  $|S_{11}|$  is less than 0.1 – 0.2 is not desirable, as for small values of  $|S_{11}|$  the corresponding measurement uncertainty is larger. The large uncertainty results from the very high sensitivity of the model to the distance between slabs and the accuracy of the slab thickness measurements.

Calculations show that the sensitivity of the measurement model can be increased by using an extended two-slab measurement model involving two slabs, one of which has a known dielectric constant, and the dielectric constant of the other slab (MUT slab) needs to be determined (measured).

In the Thesis, formulas are derived for the calculation of the scattering matrix element  $S_{11}$  and its magnitude  $|S_{11}|$ . Also, the software has been developed for calculating the sensitivity coefficient of the conventional models,  $c_{\text{cl}} = \frac{\partial |S_{11}|}{\partial \varepsilon'_{r,\text{mut}}}$ , as well as one of the extended models  $c_{\text{ex}} = \frac{\partial |S_{11}|}{\partial \varepsilon'_{r,\text{mut}}}$ . The software also solves the inverse problem to extract the dielectric constant of the MUT,  $\varepsilon'_{r,\text{mut}}$ , from a given value of  $|S_{11}|$ .

The measurement uncertainty  $u(\varepsilon'_{r,\text{mut}})$ , when  $u_{|S_{11}|}$  and other input parameter measurement uncertainties are known, can also be calculated using the developed software. Therefore, the software is capable of finding optimal dimensions of the extended models to achieve higher sensitivity than that of the conventional measurement models.

For constructing and evaluating the extended models, a procedure has been developed and validated. The proposed dielectric constant measurement procedure comprises the following six steps:

1. Insert a MUT sample with the dielectric constant to be found,  $\varepsilon'_{r,\text{mut}}$  into the rectangular waveguide, and measure the magnitude of the scattering matrix element  $|S_{11}|$ . Then from the measured value of  $|S_{11}|$ ,  $\varepsilon'_{r,\text{mut}}$  is retrieved by solving the inverse problem. Note that it is assumed that the MUT losses characterized by  $\tan \delta_{\text{mut}}$  are measured beforehand or are given in the relevant documentation.
2. Use  $\varepsilon'_{r,\text{mut}}$  calculated in the previous step, to find the sensitivity coefficient of the measurement model  $c_{\text{cl}} = \frac{\partial |S_{11}|}{\partial \varepsilon'_{r,\text{mut}}}$  and evaluate the suitability of the conventional measurement model:
  - a) if the conventional model can provide sufficiently high measurement accuracy, as the sensitivity of the model is sufficient,  $c_{\text{cl}} > 1$  (but a higher sensitivity can also be requested), then no additional measures need to be taken;
  - b) if the sensitivity of the measurement model is low,  $c_{\text{cl}} < 1$ , then an extended model

is created by adding another dielectric slab with known dimensions and dielectric constant to the MUT slab in the conventional model.

3. Select an auxiliary slab with a known dielectric constant  $\varepsilon'_{r,\text{aux}}$  and the loss tangent (it would be wiser to choose a ready-made product whose parameters are specified by the manufacturer). Find the distance between the MUT slab and the auxiliary slab,  $d_{\text{int}}$ , as well as the thickness of the additional slab,  $d_{\text{aux}}$ , which provides the highest possible sensitivity of the extended measurement model  $c_{\text{ex}} = \frac{\partial |S_{11}|}{\partial \varepsilon'_{r,\text{mut}}}$  in the range of possible values of the measured MUT dielectric constant.
4. If for the chosen auxiliary slab it is not possible to find  $d_{\text{int}}$  and  $d_{\text{aux}}$  such that the sensitivity coefficient of the extended model is sufficiently large to reach  $c_{\text{ex}}$ , then the MUT with another  $\varepsilon'_{r,\text{aux}}$  should be chosen, and Step 3 of the algorithm should be repeated.
5. To make it possible to utilize manufactured ready-to-use slabs as auxiliary slabs, an auxiliary slab is selected for the extended model whose thickness  $d_{\text{aux}}$  is closest to that calculated in Step 3.
6.  $c_{\text{ex}}$  of the created model is calculated, and in case it is sufficient, the model construction procedure is terminated.

Since it is impossible to produce auxiliary slabs with dimensions that perfectly match the calculated optimal dimensions, it is assumed that auxiliary slabs with different thickness values that differ by 0.01 mm are utilized; consequently, in Step 3 of the procedure, only these values are considered.

Numerical analysis shows that by using the method of extended models, it is practically always possible to achieve higher model sensitivity, even in those intervals of dielectric constant values, where the conventional measurement model involving only the MUT slab exhibits unacceptably low sensitivity. Numerical calculations show that for large values of  $\varepsilon'_{r,\text{mut}}$  in the central parts of the low-sensitivity regions, the improvements achieved via the use of the auxiliary slabs are not always sufficiently large and decrease with increasing  $\varepsilon'_{r,\text{mut}}$ .

In the numerical simulations of the extended two-slab model, it is assumed that the material under study is the high-frequency ceramic Arlon AD1000 [19], which is extensively employed at high-frequencies as substrates for printed antennas, filters, etc. The material has low losses at high frequencies. The data provided in the manufacturer's documentation are as follows: dielectric constant – 10.2 and loss tangent 0.003 at a frequency of 10 GHz. The documentation states that these quantities were measured by the IPC-TM-650 method [20]. In the description of the method, only the uncertainty of the dielectric constant measurements is specified, but it is not specified for the loss tangent, and therefore its value is chosen based on the average available data of other measurements.

For the auxiliary slab, the material Arlon AD430 with dielectric constant 4.3 and loss tangent equal to 0.003 is chosen [23]. This material is also widely used in various high-frequency devices

due to low losses and high thermal stability, and unlike other high-frequency ceramic materials, it is not so brittle, which simplifies mechanical processing and the sample preparation process.

It is also assumed that for both models  $|S_{11}|$  is measured using a vector network analyzer P5024B. The analyzer is assumed to be calibrated with calibration standard 85050C (TRL). The calibration method is (Full Two Port Calibrations). The measurement uncertainty after calibration is calculated using a special program Keysight VNA Uncertainty Calculator intended for evaluating the measurement uncertainty after calibration, and the calculated  $|S_{11}|$  measurement uncertainty as a function of  $|S_{11}|$  is displayed in Fig. 2.11.

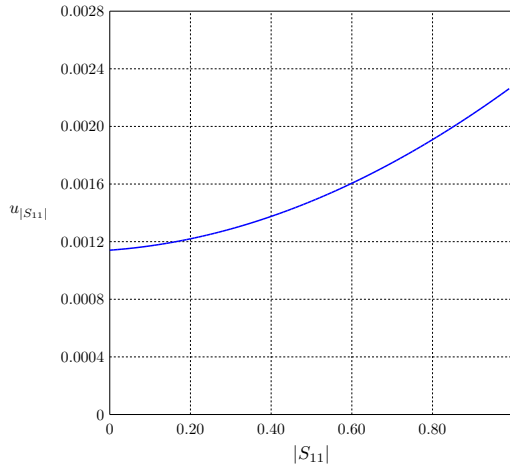


Fig. 2.11.  $u_{|S_{11}|}$  as a function of  $|S_{11}|$  for Vector Network Analyzer Keysight P5024B.

As can be seen, it increases as the value of  $|S_{11}|$  increases.

It is assumed that the thicknesses of the slabs, the width of the broader wall of the waveguide, and the distance between the slabs are measured with a digital caliper [21]. The extended measurement uncertainty of the caliper (it is specified in relevant documentation of the digital caliper) is 0.02 mm, which corresponds to the standard uncertainty of 0.01 mm.

The uncertainty of the constant dielectric measurements is evaluated using two methods: the error propagation method (EPM) and the Monte Carlo method (MCM). EPM allows for the estimation of only the standard deviation because it is based on a linear approximation of the measurement model. MCM is more accurate because it takes into account the situation when the measurement model is non-linear and estimates not only the standard uncertainty but also the mean value, which, in general, may differ from the actual value. It has been shown that even by averaging over an infinite sample of dielectric constant values, it is impossible to determine the actual value even unless the systematic component of the measurement uncertainty is completely eliminated from the model. This difference results from the non-linearity of the measurement model – the more pronounced the non-linearity, the greater the difference, and moreover, its presence is practically inevitable and unavoidable.

The parameters of the considered two-slab model are summarized in Table 2.1.

Table 2.1

Two-slab waveguide model parameters

| Model Parameter                           | Symbol                        | Value    | Uncertainty          |
|---|-------------------------------|----------|----------------------|
| MUT dielectric constant                   | $\varepsilon'_{r,\text{mut}}$ | 10.2     | –                    |
| MUT loss tangent                          | $\tan \delta_{\text{mut}}$    | 0.0023   | $1.15 \cdot 10^{-4}$ |
| Dielectric constant of the auxiliary slab | $\varepsilon'_{r,\text{aux}}$ | 4.3      | 0.043                |
| Auxiliary slab loss tangent               | $\tan \delta_{\text{aux}}$    | 0.003    | $5.0 \cdot 10^{-5}$  |
| MUT slab thickness                        | $d_{\text{mut}}$              | 2.5 mm   | 0.01 mm              |
| Auxiliary slab thickness                  | $d_{\text{aux}}$              | 3.8 mm   | 0.01 mm              |
| Interslab distance                        | $d_{\text{int}}$              | 20 mm    | 0.01 mm              |
| Frequency                                 | $f$                           | 10 GHz   | 35 MHz               |
| Waveguide width                           | $a$                           | 22.86 mm | 0.01 mm              |

Figure 2.12 shows  $|S_{11}|$  as a function  $\varepsilon'_{r,\text{mut}}$ , and the widths of the confidence intervals calculated for the conventional (KMMVM) and extended (DMMVM) models. As can be seen, the extended model gives about 6.2 times smaller width of the confidence interval than in the case of the conventional model. This is a good justification for the chosen approach, which is based on reducing the measurement uncertainty via extending conventional measurement models.

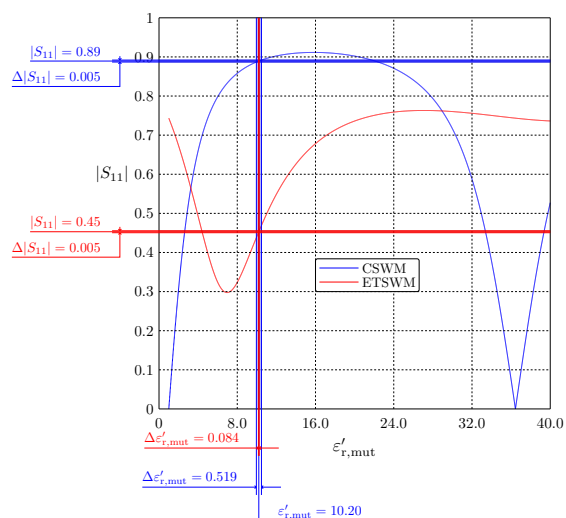


Fig. 2.12.  $|S_{11}|$  as a function of  $\varepsilon'_{r,\text{mut}}$  and the widths of confidence intervals for conventional (CSWM) and for extended (ETSWM) models.

Figure 2.13 shows the standard uncertainty as a function of  $\varepsilon'_{r,\text{mut}}$  for the conventional (KMMVM) and extended (DMMVM) models. The missing regions of the curve correspond to mea-

surement model parameter value ranges where the MCM estimation fails. This failure results from the fact that for more than 10 % of the MCM realizations  $|S_{11}|$  takes values greater than the maximum possible  $|S_{11}|$ . The maximum value of  $|S_{11}|$ , in turn, is determined by the definition of this quantity, as well as VNA capabilities. Such situations arise when the MCM method is employed, and the actual value of the dielectric constant lies in a low-sensitivity region of the measurement model.

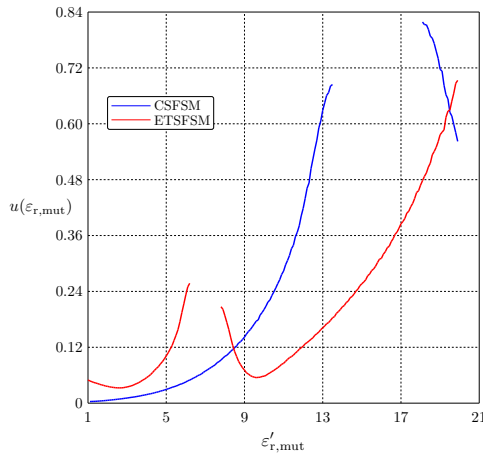


Fig. 2.13. The standard uncertainty as a function of  $\epsilon'_{r,mut}$  for the conventional (CSWM) and the extended (ETSWM) models.

Section 3.3 describes the generalization of the two-slab model, namely, the three-slab model. Although it was previously concluded that the sensitivity of the measurement model could be increased using a relatively simple two-slab model, when the measurements are to be performed for a fixed slab thickness (non-destructive measurement) at a fixed frequency, this model has a number of shortcomings that manifest themselves in the practical realization of the model.

One of the disadvantages of the two-slab model is the problem of ensuring the optimal separation between slabs, since, in practice, it is difficult to position the slabs so that the distance between them is equal to the calculated optimal distance, and it is also difficult to measure this distance.

Additional problems are caused by the fact that slabs with a small thickness are very difficult to place so that their broader faces are normal to the wave propagation direction. Even a slight shift in the slab position can cause a difference between the calculated and measured results. This circumstance is less important when measuring relatively thick slabs, but in such a model, the air gaps between the slab faces and the waveguide walls and their effect on the measurement results must be taken into account – the greater the thickness of the slab, the greater the effect of the air-gap on the measurement accuracy. In practice, the effect of the air gap is typically reduced by using special pastes with high conductivity.

In order to mitigate the above-mentioned problem, the author proposes to use a three-slab

model (see Fig. 2.14), in which, in contrast to the two-slab model, there is another dielectric auxiliary slab between the two slabs (the auxiliary slab and the slab to be measured). The slabs in this model are arranged so that there are no air gaps between them. The main advantage of the three-slab model is the ability to establish the thickness of the middle slab and, therefore, the distance between the outer slabs with higher accuracy.

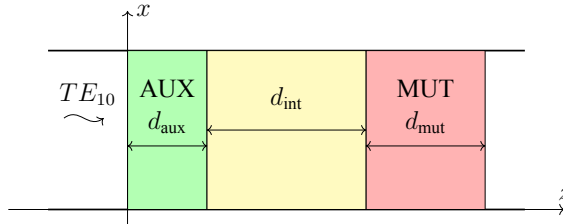


Fig. 2.14. The geometry of the three-slab waveguide measurement model.

In the analysis of the extended model, it is assumed that slab thickness could not take arbitrary values for the selection of the optimal case. To make it possible to test the model experimentally, the thickness of the auxiliary slabs in the extended three-slab model may take only a discrete set of values with the step size of 0.01 mm, so that it would be possible to create these slabs with the calculated thicknesses.

The calculated parameters of the constructed extended three-slab model with improved sensitivity, including the MUT parameters, are summarized Table 2.2.

Table 2.2

Three-slab waveguide model parameters

| Model Parameter                           | Symbol              | Value    | Uncertainty          |
|---|---------------------|----------|----------------------|
| MUT dielectric constant                   | $\epsilon'_{r,mut}$ | 10.2     | –                    |
| MUT loss tangent                          | $\tan \delta_{mut}$ | 0.0023   | $1.15 \cdot 10^{-4}$ |
| Dielectric constant of the auxiliary slab | $\epsilon'_{r,aux}$ | 4.3      | 0.043                |
| Auxiliary slab loss tangent               | $\tan \delta_{aux}$ | 0.003    | $5.0 \cdot 10^{-5}$  |
| Dielectric constant of the middle slab    | $\epsilon'_{r,int}$ | 2.2      | 0.022                |
| Middle slab loss tangent                  | $\tan \delta_{int}$ | 0.0009   | $5.0 \cdot 10^{-5}$  |
| MUT slab thickness                        | $d_{mut}$           | 2.5 mm   | 0.01 mm              |
| Auxiliary slab thickness                  | $d_{aux}$           | 7.0 mm   | 0.01 mm              |
| Middle slab thickness                     | $d_{int}$           | 7.1 mm   | 0.01 mm              |
| Frequency                                 | $f$                 | 10 GHz   | 35 MHz               |
| Waveguide width                           | $a$                 | 22.86 mm | 0.01 mm              |

Figure 2.15 shows  $|S_{11}|$  as a function of  $\epsilon'_{r,mut}$ , and the widths of the confidence intervals for the conventional (KMMVM) and the extended three-slabs (TMMVM) models. As can be seen, the extended model gives about 2.5 times smaller confidence interval width.

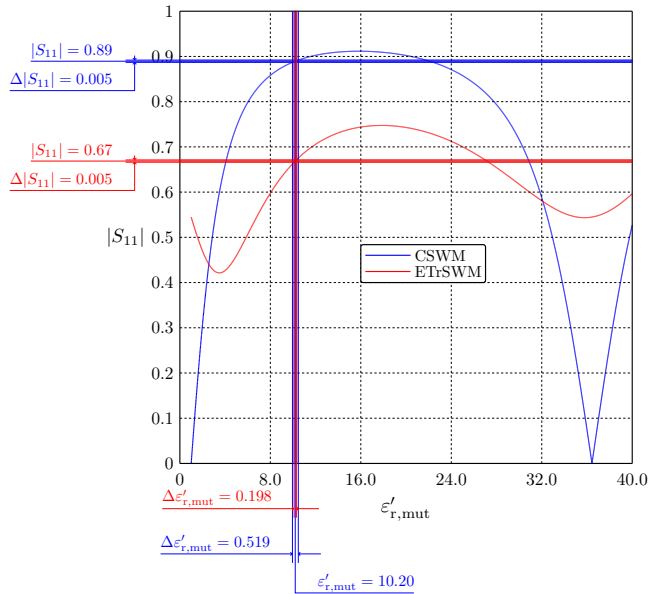


Fig. 2.15.  $|S_{11}|$  as a function of  $\epsilon'_{r,\text{mut}}$  and the widths of the confidence intervals for the conventional (CSWM) and the extended (ETrSWM) models.

Figure 2.16 presents the standard dielectric constant measurement uncertainty plotted against  $\epsilon'_{r,\text{mut}}$  for the conventional (KMMVM) and extended (TMMVM) models.

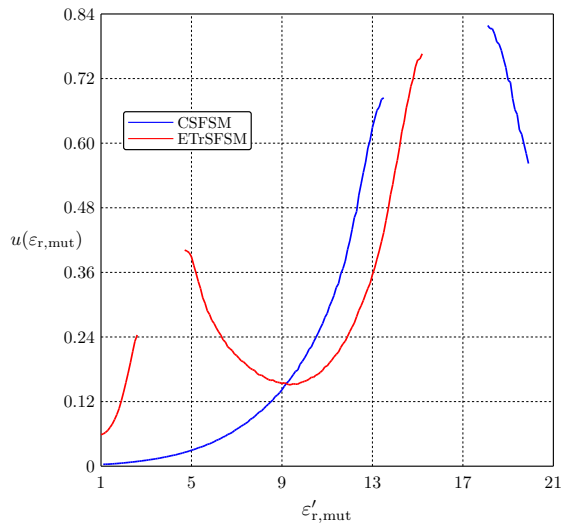


Fig. 2.16. The standard uncertainty as a function of  $\epsilon'_{r,\text{mut}}$  for the conventional (CSWM) and the extended (ETrSWM) models.

## 2.4. Extended Multi-slab Measurement Models for the Free Space Method

Chapter 4 of the Thesis describes the construction, analysis, and optimization of extended free space slab measurement models.

It is assumed that the incident wave is a plane wave and that the dielectric slabs have an infinite width and height. In the measurement model being examined, the wave is incident on the slabs perpendicular to their surface (normal incidence). These assumptions significantly simplify the analysis, since the analytical mathematical expressions can be used for the calculation of  $|S_{11}|$ .

The free space method is widely used in non-destructive measurements of slabs. However, the method does not ensure high accuracy, as in real-life measurements, slabs of finite transverse dimensions must be used. For the method to provide adequate measurement accuracy, the MUT slab transverse dimensions (slab width and height) must be sufficiently large. In the scientific literature, it is generally considered sufficient that the width and height of the slabs should be at least three wavelengths. If the dimensions of the sample are not sufficiently large, the slab edge diffraction effect may significantly affect measurement results. Nevertheless, there are effective techniques to reduce the diffraction effects, e.g., placing ferrite absorbers at the edges of the sample.

As before, it is assumed that measurements are made with a calibrated VNA P5024B (two-port calibration method). For this measurement device, the uncertainty of the reflection coefficient is, on average, around 0.003.

In Section 4.2. the two-slab model of the free space method is studied. In the calculation example, a high-frequency ceramic with the actual value of the dielectric constant of 30 and the loss tangent of  $6.67 \cdot 10^{-5}$  is chosen as the material to be measured [22]. Dielectric material Arlon AD1000 [19] with a dielectric constant of 10.2 and a loss tangent equal to 0.0023 is chosen for the auxiliary slab. The geometry of the two-slab model under consideration is shown in Fig. 2.17.

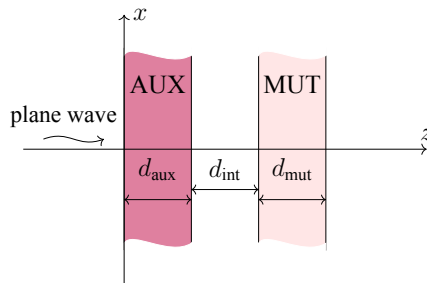


Fig. 2.17. The geometry of the two-slab free space measurement model.

Parameter estimation for the two-slab free space measurement model was performed to improve the sensitivity of the conventional model. The calculated parameters of the measurement model are presented in Table 2.3.

Table 2.3

Two-slab free space model parameters

| Model Parameter                           | Symbol                        | Value                | Uncertainty          |
|---|-------------------------------|----------------------|----------------------|
| MUT dielectric constant                   | $\varepsilon'_{r,\text{mut}}$ | 30                   | —                    |
| MUT loss tangent                          | $\tan \delta_{\text{mut}}$    | $6.67 \cdot 10^{-5}$ | $3.33 \cdot 10^{-6}$ |
| Dielectric constant of the auxiliary slab | $\varepsilon'_{r,\text{aux}}$ | 10.2                 | 0.0102               |
| Auxiliary slab loss tangent               | $\tan \delta_{\text{aux}}$    | 0.0023               | $5.0 \cdot 10^{-5}$  |
| MUT slab thickness                        | $d_{\text{mut}}$              | 2.0 mm               | 0.01 mm              |
| Auxiliary slab thickness                  | $d_{\text{aux}}$              | 2.6 mm               | 0.01 mm              |
| Interslab distance                        | $d_{\text{int}}$              | 13.1 mm              | 0.01 mm              |
| Frequency                                 | $f$                           | 10 GHz               | 35 MHz               |

Figure 2.18 shows  $|S_{11}(\varepsilon'_{r,\text{mut}})|$  as a function  $\varepsilon'_{r,\text{mut}}$  for the conventional and the extended models, as well as the corresponding measurement uncertainties. As can be observed, the sensitivity of the extended model is considerably higher (which in this case is approximately 5.8 times higher), thereby resulting in a significant reduction of the MUT dielectric constant measurement uncertainty  $u(\varepsilon'_{r,\text{mut}})$ .

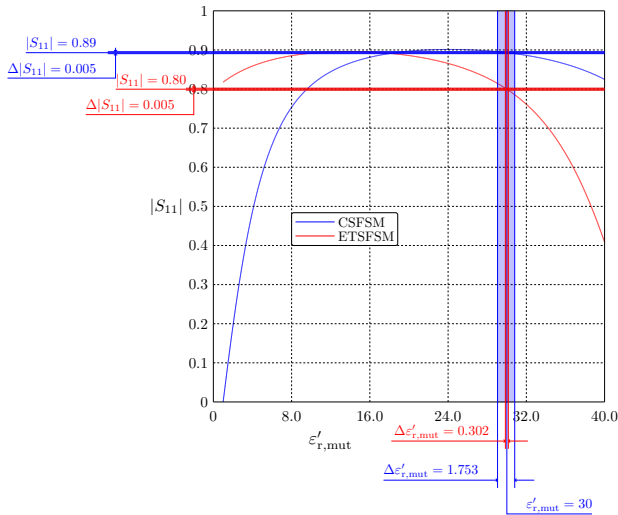


Fig. 2.18.  $|S_{11}|$  as a function of  $\varepsilon'_{r,\text{mut}}$ , and the confidence interval widths for the conventional (CSFSM) and the extended (ETSFSM) models.

Figure 2.19 shows  $u(\varepsilon'_{r,\text{mut}})$  plotted as a function  $\varepsilon'_{\text{extr},\text{mut}}$  of the MUT dielectric constant for the conventional and extended models. The explanation of the results is similar to that for the results in Fig. 2.13.

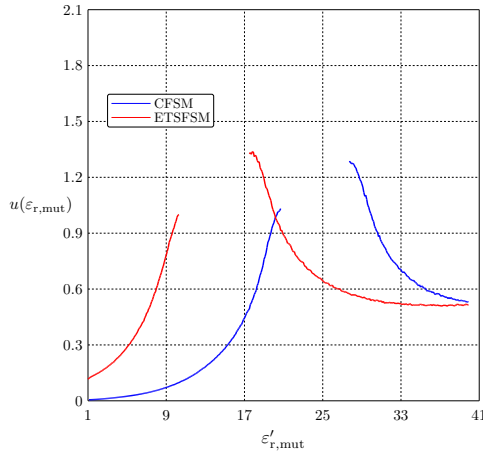


Fig. 2.19. The standard uncertainty as a function of the interslab distance for the conventional (CSFSM) and the extended (ETSFSM) models.

Section 4.2 discusses a generalization of the two-slab free space model – a three-slab model. Similar to the waveguide model, the free-space two-slab model also allows for achieving a higher sensitivity of the measured quantity  $|S_{11}|$  to small variations in the interslab distance than that of the conventional free-space model involving a single slab only. However, due to the fact that the size of the sample, in this case, is sufficiently large, this problem can be mitigated with the aid of specialized sample holders designed to ensure relatively accurate positioning of the slabs but are, unfortunately, quite expensive equipment and would be more costly. In this case, a solution similar to that for the waveguide model is proposed and studied. The study is similar to that of the three-slab waveguide model – an additional dielectric slab is placed between the main slabs. The slabs are arranged so that there are no gaps between them.

The geometry of the three-slab model under consideration is illustrated in Fig. 2.20.

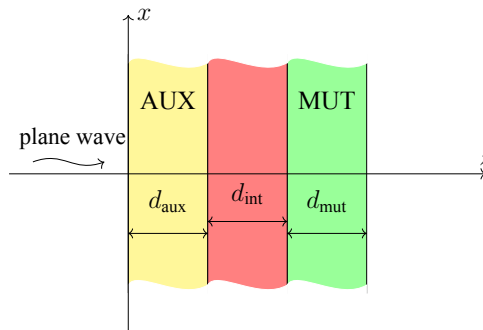


Fig. 2.20. The geometry of the three-slab free space measurement model.

The model parameter estimation for the extended free-space three-slab measurement model was performed with a view to improving the sensitivity of the conventional model. The param-

eters of the model known as a result of the calculation are summarized in Table 2.4.

Table 2.4

Three-slab free space model parameters

| Model Parameter                           | Symbol              | Value                | Uncertainty          |
|---|---------------------|----------------------|----------------------|
| MUT dielectric constant                   | $\epsilon'_{r,mut}$ | 30                   | –                    |
| MUT loss tangent                          | $\tan \delta_{mut}$ | $6.67 \cdot 10^{-5}$ | $3.33 \cdot 10^{-6}$ |
| Dielectric constant of the auxiliary slab | $\epsilon'_{r,aux}$ | 10.2                 | 0.0102               |
| Auxiliary slab loss tangent               | $\tan \delta_{aux}$ | 0.0023               | $5 \cdot 10^{-5}$    |
| Dielectric constant of the middle slab    | $\epsilon'_{r,int}$ | 2.2                  | 0.022                |
| Middle slab loss tangent                  | $\tan \delta_{int}$ | 0.0009               | $5 \cdot 10^{-5}$    |
| MUT slab thickness                        | $d_{mut}$           | 2.4 mm               | 0.01 mm              |
| Auxiliary slab thickness                  | $d_{aux}$           | 5.7 mm               | 0.01 mm              |
| Middle slab thickness                     | $d_{int}$           | 9.6 mm               | 0.01 mm              |
| Frequency                                 | $f$                 | 10 GHz               | 35 MHz               |

Figure 2.21 shows  $|S_{11}(\epsilon'_{r,mut})|$  as a function of  $\epsilon'_{r,mut}$  and the corresponding measurement uncertainties for the conventional and extended three-slab models. From the figure, it is evident that the sensitivity of the expanded model (its parameters are presented in Table 2.4) is appreciably higher. The result is a considerable reduction in the MUT dielectric constant measurements uncertainty,  $u(\epsilon'_{r,mut})$ , which in this case is approximately 3.5 times smaller than in the case of the conventional model.

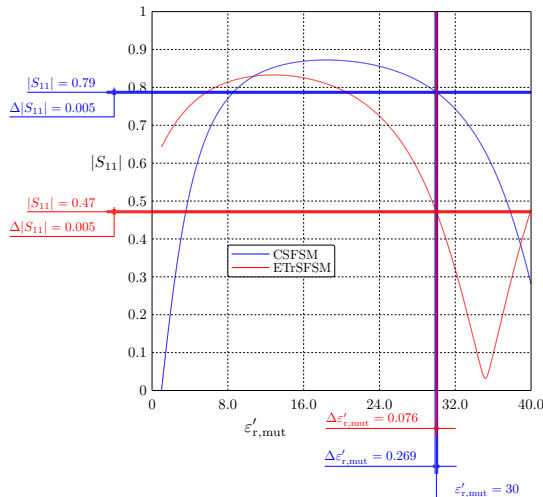


Fig. 2.21.  $|S_{11}|$  as a function of  $\epsilon'_{r,mut}$ , and the confidence interval widths for the conventional (CSFSM) and the extended (ETrSFSM) models.

It is worth noting that the increase in the measurement sensitivity achieved with the use of the extended models and the corresponding reduction in the measurement uncertainty compared

to the conventional model becomes smaller as  $\varepsilon'_{r,\text{mut}}$  increases, which in this case is 30.0. Thus, in measuring the MUT with a low dielectric constant, the three-slab models outperform their conventional counterparts in measurement accuracy, which is an undeniable advantage of the extended models.

Figure 2.22 indicates the measurement uncertainty,  $u(\varepsilon'_{r,\text{mut}})$ , as a function of  $\varepsilon'_{r,\text{mut}}$  for the conventional and extended three-slab model MUT. However, in constant to its two-slab counterpart, the three-slab model fails to provide smaller measurement uncertainty, even though its model sensitivity is considerably higher.

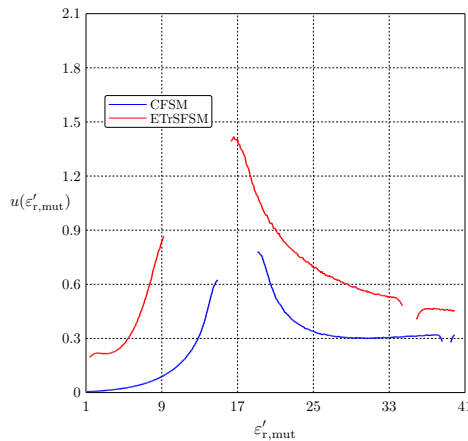


Fig. 2.22. The standard uncertainty as a function of the interslab distance for the conventional (CSFSM) and the extended (ETrSFSM) models.

## 2.5. Extended Two-Rod Measurement Model for the Waveguide Method

Chapter 5 of the Thesis describes the construction, optimization, and analysis of extended measurement models involving two cylindrical dielectric rods in a rectangular waveguide. One of these rods is made of a low-loss material under investigation (MUT) whose dielectric constant is to be determined from the measured  $|S_{11}|$ . The second rod is an auxiliary rod whose dimensions and material properties are known a priori (found by means of the model optimization procedure). Measurements are performed at a fixed frequency chosen so that only the dominant mode can propagate in the waveguide. The distance between the rods and the radius of the auxiliary rod are treated as model optimization parameters. The fast integral equation method developed by the author is utilized to solve the forward scattering problem, as it gives accurate results while requiring significantly less computing time than other methods. The fast calculation method is described in Chapter 6.

The geometry of the two-rod waveguide model is shown in Fig. 2.23. The parameters of the two-rod measurement model under study are summarized in Table 2.5.

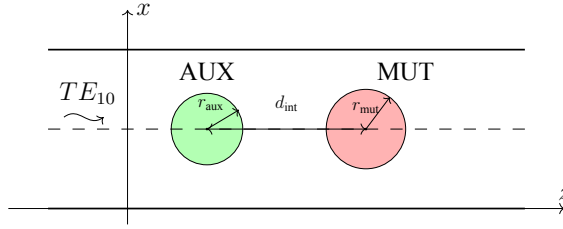


Fig. 2.23. The geometry of the extended two-rod waveguide measurement model.

Table 2.5

Two-rod waveguide model parameters

| Model Parameter                          | Symbol              | Value    | Uncertainty          |
|--|---------------------|----------|----------------------|
| MUT dielectric constant                  | $\epsilon'_{r,mut}$ | 10.2     | –                    |
| MUT loss tangent                         | $\tan \delta_{mut}$ | 0.0023   | $1.15 \cdot 10^{-4}$ |
| Dielectric constant of the auxiliary rod | $\epsilon'_{r,aux}$ | 4.3      | 0.043                |
| Auxiliary rod loss tangent               | $\tan \delta_{aux}$ | 0.003    | $5.0 \cdot 10^{-5}$  |
| MUT rod radius                           | $r_{mut}$           | 2.5 mm   | 0.01 mm              |
| Auxiliary rod radius                     | $r_{aux}$           | 5.7 mm   | 0.01 mm              |
| Interrod distance                        | $d_{int}$           | 8.6 mm   | 0.01 mm              |
| Frequency                                | $f$                 | 10 GHz   | 35 MHz               |
| Waveguide width                          | $a$                 | 22.86 mm | 0.01 mm              |

Figure 2.24 shows the calculated  $|S_{11}|$  as a function of  $\epsilon'_{r,mut}$  and the corresponding measurement uncertainties.

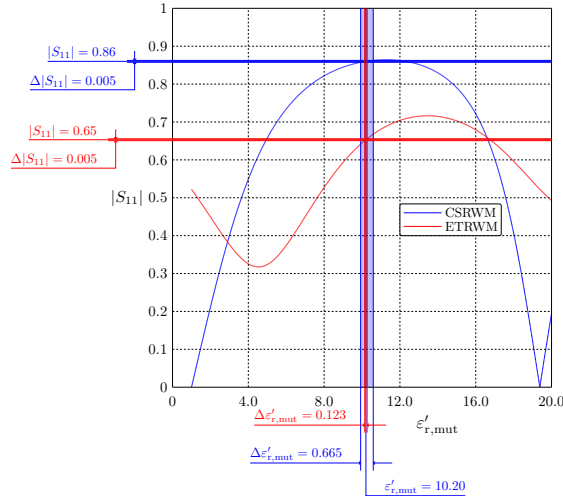


Fig. 2.24.  $|S_{11}|$  as a function of  $\epsilon'_{r,mut}$  and the confidence intervals for the conventional (CSRWM) and the extended (ETRWM) models.

The measurement uncertainty  $u(\varepsilon'_{r,\text{mut}})$  of the extended model (model parameters are summarized in Table 2.5) is appreciably smaller than that of the conventional model (measured by MUT  $\varepsilon'_{r,\text{mut}}$ ).

Note that the computation time required for the forward problem solving ( $|S_{11}(\varepsilon'_{r,\text{mut}})|$ ) for models involving rods in the waveguide is considerably larger than for models with slabs in the waveguide. Without the fast integral equation method developed by the author (described in Chapter 6), the MCM-based measurement uncertainty analysis for the two-rod model would be practically impossible due to the prohibitively large computational burden.

The measurement uncertainty  $u(\varepsilon'_{r,\text{mut}})$  as a function of  $\varepsilon'_{r,\text{mut}}$  calculated for the conventional (MUT only) and extended three-slab models is shown in Fig. 2.25. The discussion of the results obtained for this model is similar to that in Fig. 2.13. In addition, the results displayed in this figure clearly show that there are several ranges of the dielectric constant values (low sensitivity regions), where it is practically impossible to make adequate dielectric constant measurements.

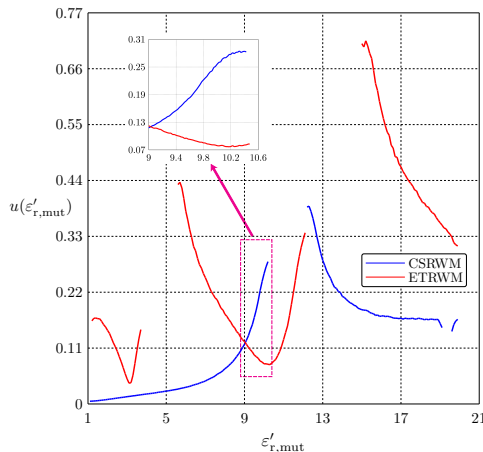


Fig. 2.25. The standard uncertainty as a function of  $\varepsilon'_{r,\text{mut}}$  for the conventional (CSRWM) and the extended (ETRWM) models.

## 2.6. Fast Integral Equation Method

Chapter 6 of the Thesis describes a fast and accurate method developed by the author to analyze the multi-rod waveguide measurement model. The model is composed of two circular cylindrical dielectric rods, one of which is made of the MUT, while the other one has known CP and is intended for the optimization of the measurement model. The rods are arranged so that their axes are parallel to the side walls of the waveguide. Calculations and a comparative analysis carried out herein demonstrated that the computational method developed by the author significantly accelerates the measurement uncertainty estimation process, as it is capable of calculating the forward scattering problem considerably faster than existing commercially available software, such as Ansys HFSS.

The proposed calculation method is, in essence, the boundary surface integral equation method. Both weighting and basis functions are approximated by sufficiently simple functions such as polynomials. However, if the considered object has a simple (canonical) shape, such as cylindrical, spherical or elliptical, the fields on the surfaces can be expressed in terms of the so-called Entire Domain Basis Functions, which are typically, solutions to the relevant differential equation, as well as satisfy the relevant boundary conditions, e.g., for the treatment of cylindrical objects the most suitable conditions are the periodic ones, as they are completely natural.

In the proposed method, the integral equations relating the fields on the rod surfaces are discretized and for the resulting integrals to be evaluated to determine the system matrix entries can be evaluated analytically. However, the integration results in infinite Schlömilch series that converge very slowly, thereby significantly deteriorating the overall efficiency of the method. To overcome this problem, one needs to speed up the convergence of these series, which in the present Thesis is achieved by using the Ewald method [24] that for a long time has mainly been utilized to accelerate the calculation of periodic lattice potentials, and only recently it has gained popularity in the microwave community, as it proves to be one of the most efficient methods for the calculations of Schlömilch series along the same lines. It is assumed that the waveguide is operated in a single-mode regime. A possible geometry of the structure under consideration is shown in Fig. 2.26. In the general case the rectangular waveguide contains  $P$  layered or solid rods and  $p_i$  refers to the number of layers of the  $i$ -th cylinder.

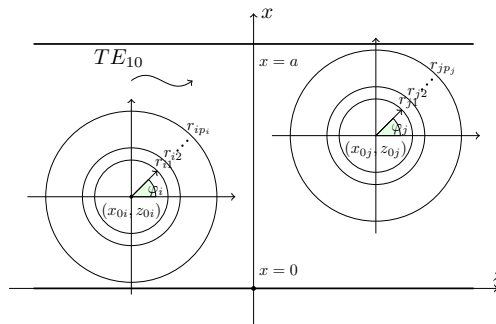


Fig. 2.26. An example of the considered structures – two layered cylinders in a rectangular waveguide [25].

The waveguide is assumed to operate in a mode where only the dominant mode can propagate in it. To find the fields resulting from the interaction of the dominant mode with the set of rods, the following surface integral equation must be solved:

$$E_y^i(\mathbf{r}_o) = E_y(\mathbf{r}_o) - \oint_L \left( E_y(\mathbf{r}_s) \frac{\partial G(\mathbf{r}_o, \mathbf{r}_s)}{\partial n} + jZ_0 k_0 H_\varphi(\mathbf{r}_s) G(\mathbf{r}_o, \mathbf{r}_s) \right) dl_s, \quad (2.5)$$

where

$G(\mathbf{r}_o, \mathbf{r}_s)$  – the Green's function of the waveguide;

$E_y^i(\mathbf{r}_s)$  – the incident electric field, V/m;

$Z_0$  – the free space intrinsic impedance,  $\Omega$ ;

$k_0$  – the wave number in free space,  $1/\text{m}$ ;

$E_y(\mathbf{r})$  – the tangential components of the total electric field,  $\text{V/m}$ ;

$H_\varphi(\mathbf{r})$  – the tangential components of the total magnetic field,  $\text{A/m}$ .

Here, the Green's function and the above fields are only considered on the rod surfaces,  $L = \{L_1 \cup \dots \cup L_P\}$ , where  $L_i$  is  $i$ -th rod surface.

In order to find the unknown functions  $E_y(\mathbf{r})$  and  $H_\varphi(\mathbf{r})$ , it is necessary to transform the Equation (3.3) into the so-called weak form by multiplying both sides of the equation with testing functions  $T_{h,\{i\}}(\varphi_{\{i\}}) = e^{-jh\varphi_{\{i\}}}$ ,  $h = -N, -N+1, \dots, N$  and integrating over each  $L_i$ ,  $i = 1, 2, \dots, P$ .

Then, by approximating the electric  $E_y(r_{\{j\}}, \varphi_{\{j\}})$  and the magnetic  $H_\varphi(r_{\{j\}}, \varphi_{\{j\}})$  fields on the surface of the  $j$ -th cylinder with the basis functions  $e^{jn\varphi_{\{i\}}}$ ,  $n = -N, -N+1, \dots, N$  with unknown expansion coefficients  $\tilde{E}_{n,\{j\}}$  and  $\tilde{H}_{n,\{j\}}$ , one eventually obtains the following expressions for the coefficients of the system matrix submatrices  $\mathbf{Z}_{ij}^H$  and  $\mathbf{Z}_{ij}^E$

$$\begin{aligned} z_{ij;(h+N+1)(n+N+1)}^H &= -jZ_0 \left( S_{n-h}^- - (-1)^n S_{-(n+h)}^+ \right) J_h(k_0 r_{0,\{i\}}) J_n(k_0 r_{0,\{j\}}), \\ z_{ij;(h+N+1)(n+N+1)}^E &= \left( S_{n-h}^- - (-1)^n S_{-(n+h)}^+ \right) J_h(k_0 r_{0,\{i\}}) J'_n(k_0 r_{0,\{j\}}), \end{aligned} \quad (2.6)$$

where

$S_l^\pm = jk_0 \pi^2 r_{0,\{i\}} r_{0,\{j\}} \sum_{m=-\infty}^{+\infty} H_l^{(2)}(k_0 r_{m,i,j}^\pm) e^{jl\varphi_m^\pm}$  – the Schlömilch series of the  $l$ -th order;

$r_{0,\{i\}}$  – radius of the  $i$ -th rod,  $\text{m}$ ;

$J_n(x)$  –  $n$ -th order Bessel function;

$H_n^{(2)}(x)$  –  $n$ -th order Hankel function of the second kind;

$r_{m,i,j}^\pm = \sqrt{(x_{0,\{i\}} \pm x_{0,\{j\}} + 2am)^2 + (z_{0,\{i\}} - z_{0,\{j\}})^2}$ ;

$\varphi_m^\pm = \arctan((x_{0,\{i\}} \pm x_{0,\{j\}} + 2am)/(z_{0,\{i\}} - z_{0,\{j\}}))$ .

By solving the resulting system of equations, the approximation coefficients of the fields are obtained, from which the elements of the scattering matrix can be easily obtained by integrating over the surface of each cylinder. In this case, the integrals can be found analytically using the Jacobi-Anger expansion. It is worth noting that the expansion converges not only for the real angles but also for the complex angles, which arise when calculating the generalized scattering parameters. To accelerate the series evaluation, the initial series is divided into two sub-series, one being rapidly converging, whereas the other series converges dramatically slowly but can be significantly accelerated by means of the Poisson summation method. The expressions  $S_l^+$  and  $S_l^-$  can be obtained from the expressions  $S_0^+$  and  $S_0^-$  using recursions formulas for Hankel functions [24].

To find the relation between the tangential components of the magnetic and electric fields on the surface of the  $j$ -th rod, the fields in the rod layers are expressed in terms of a series of cylindrical functions, since these functions satisfy the homogeneous Helmholtz equation in the

cylindrical coordinate system and are therefore the most suitable for field approximations in the present case. The relation between the field approximation coefficients  $A_{n,\{j\}}$  and  $B_{n,\{j\}}$  can be found by equating the tangential components of the fields on the surface of the  $j$ -th rod layer and exploiting the orthogonality with respect to  $\varphi_{\{j\}}$ . By doing so, one obtains infinitely many systems of uncoupled equations, each of which includes only the  $n$ -th unknown coefficient for all layers of the rod. Then,  $g_{n,\{j\}} = B_{n,\{j\}}/A_{n,\{j\}}$  is found using the following recurrence relation obtained by successively eliminating all the unknown expansion coefficients except for  $A_{n,\{j\}}$  and  $B_{n,\{j\}}$  from the  $n$ -th set of equations, starting with the inner layer:

$$g_{n,\{j,o\}} = \frac{\tilde{k}_{\{j,o\}} J_{n-1}(\tilde{k}_{\{j,o\}}) Q_{n,\{j,o\}}(\tilde{k}_{\{j,(o-1)\}}) - \tilde{k}_{\{j,(o-1)\}} J_n(\tilde{k}_{\{j,o\}}) Q_{(n-1),\{j,o\}}(\tilde{k}_{\{j,(o-1)\}})}{\tilde{k}_{\{j,(o-1)\}} Y_n(\tilde{k}_{\{j,o\}}) Q_{(n-1),\{j,o\}}(\tilde{k}_{\{j,(o-1)\}}) - \tilde{k}_{\{j,o\}} Y_{n-1}(\tilde{k}_{\{j,o\}}) Q_{n,\{j,o\}}(\tilde{k}_{\{j,(o-1)\}})}, \quad (2.7)$$

where

$$Q_{n,\{j,o\}}(x) = J_n(x) + g_{n,\{j,(o-1)\}} Y_n(x);$$

$$\tilde{k}_{\{j,l\}} = k_{\{j,l\}} r_{\{j,(o-1)\}};$$

$$g_{n,\{j,1\}} = 0;$$

$k_{\{j,o\}}$  – the wavenumber in the  $o$ -th layer of the  $j$ -th rod;

$A_{n,\{j,o\}}$  and  $B_{n,\{j,o\}}$  – unknown approximation coefficients.

To accelerate the convergence of the Schlömilch series, the integral along the imaginary axis is divided into two integrals via deforming the integration contour. This approach results in two rapidly converging series. In this case, the parameter  $\alpha$  is a positive real number that allows for controlling the convergence of the two series. The integration contour is deformed so that the resulting one comprises two straight line segments, one of which is the segment of a straight line joining the origin and the point that corresponds to number  $\alpha^2$ , whereas the second one is a ray emerging from point  $\alpha^2$  and extends to infinity in the direction of the imaginary axis. To validate the method,  $|S_{11}|$  was calculated for the structure depicted in Fig. 2.27. The parameters of the structure under consideration are presented in Table 2.6. The calculation results are shown in Fig. 2.28, and the calculation times are summarized in Table 2.7.

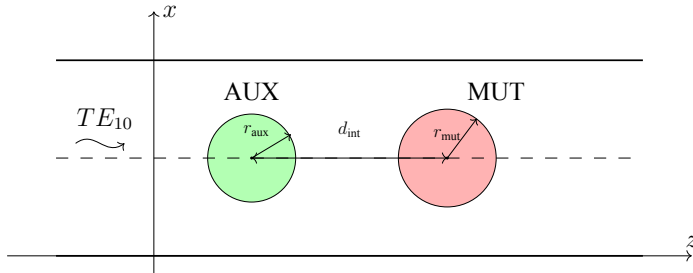


Fig. 2.27. Two dielectric rods in a rectangular waveguide.

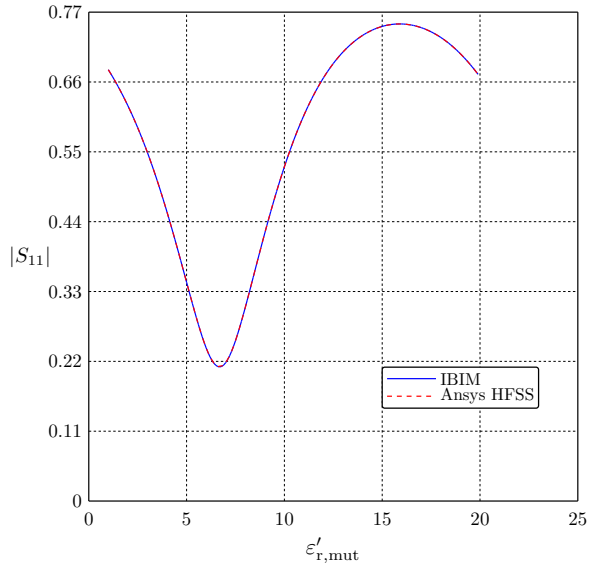


Fig. 2.28.  $|S_{11}|$  as a function of  $\epsilon'_{r,mut}$  calculated using the proposed method (IBIM) and the Ansys HFSS.

Table 2.6

Parameters of the two-rod model

| Model Parameter                          | Symbol              | Value    |
|--|---------------------|----------|
| MUT dielectric constant                  | $\epsilon'_{r,mut}$ | 10.2     |
| MUT loss tangent                         | $\tan \delta_{mut}$ | 0.0023   |
| Dielectric constant of the auxiliary rod | $\epsilon'_{r,aux}$ | 4.3      |
| Auxiliary rod loss tangent               | $\tan \delta_{aux}$ | 0.003    |
| MUT rod radius                           | $r_{mut}$           | 2.5 mm   |
| The radius of the auxiliary rod          | $d_{aux}$           | 6.5 mm   |
| Interrod distance                        | $r_{int}$           | 27.5 mm  |
| Frequency                                | $f$                 | 10 GHz   |
| Waveguide width                          | $a$                 | 22.86 mm |

Table 2.7

Comparison of computation times

| Model Parameter | Symbol |
|-----------------|--------|
| Method          | Time s |
| IBIM            | 8.2    |
| Ansys HFSS      | 824.6  |

## CONCLUSIONS

The Thesis is dedicated to the evaluation and sensitivity improvement of dielectric constant measurement models for high-frequency low-loss dielectric materials. Several of the most widely used dielectric constant measurement models have been investigated: 1) a model where the material under test (MUT) is a dielectric slab in a rectangular waveguide or free space; 2) a model where the MUT is a cylindrical dielectric rod in a waveguide. Both measurement models employ the reflection technique to retrieve dielectric constant. The main result of the research is a simple, fast, and convenient measurement model evaluation methodology, which can be applied even when model parameters (MUT dimensions, frequency, as well as the expected value of the dielectric constant) cannot be altered. In the case when the model sensitivity is unacceptably low, and the model parameters are not allowed to be changed, e.g., when it is required by standards or measurements have to be non-destructive or made at a fixed frequency, the author has developed several measurement models employing additional dielectric objects alongside the MUT. To facilitate the construction and calculation of the improved measurement models, the author has developed a number of analytical and numerical approaches. The author has also developed a new numerical method for the analysis of models with a single or multiple circular cylindrical rods in a waveguide, the use of which results in an appreciable reduction in the computation time compared to the existing general-purpose numerical methods, which is essential when the measurement uncertainty is estimated with the use of the Monte Carlo method.

1. In the Thesis, it is shown and numerically verified that the measurement model sensitivity depends significantly on model parameter values and that in the case when the measurements are to be performed at a fixed frequency and for the MUT whose shape cannot be changed, the model sensitivity is significantly affected by the dielectric constant. Also, it is shown that there are dielectric constant value ranges where the model sensitivity is very low, resulting in unacceptably large measurement uncertainties. Furthermore, these low-sensitivity regions become very wide for the MUT dielectric constant values greater than approximately 10.
2. A new methodology is proposed that allows one to evaluate the sensitivity of dielectric constant measurement models based on the data obtained by solving the forward scattering problem only, which makes it possible to quickly and straightforwardly evaluate whether the model is suitable for measurements or not.
3. In the Thesis, it is demonstrated and numerically verified that in the case when the measurements must be performed for a fixed set of model parameters and it is found that the conventional model is not suitable due to an unacceptably large measurement uncertainty; it is possible to construct another non-destructive measurement model to reduce the measurement uncertainty. This model can be constructed by adding one or more additional elements to the conventional model containing the MUT only. Additionally, it is demonstrated that the model sensitivity can also be improved by changing the dimensions of the

sample, but this would require sample destruction, which is not always permissible and possible.

4. The following new models were developed for the extended measurement models:
  - in case a measurement method that involves measuring the dielectric constant of a slab made of the MUT and located in free space or a waveguide is employed, the new models are the two-slab model and the three-slab model;
  - in case a measurement method that involves measuring the dielectric constant of a cylindrical rod made of the MUT (it can be hollow in the middle) and located in a rectangular waveguide is employed, the new measurement model is constructed by adding an auxiliary cylindrical rod.
5. It has been shown that even when conventional measurement models do not exhibit sufficiently high model sensitivity, an extended measurement model developed by the author can be used to considerably improve it (at least 3–5 times) to reduce the dielectric constant measurement uncertainty.
6. The author has developed, successfully verified, and employed for the analysis of some of the measurement models examined in the Thesis a new fast and accurate integral equation based numerical method for the scattering data calculation for structures composed of one or more multilayered circular cylindrical dielectric rods, as well as metallic rods. The method has been shown to compute the scattering data at least 50 times faster than existing commercially available finite-element-based software.

The results presented in the Thesis have been approved and show that all research objectives of the Doctoral Thesis have been achieved, and all planned analytical and numerical studies have been successfully accomplished. The results may be of particular importance for the evaluation of dielectric constant measurement models for low-loss dielectric materials and for constructing new models with a higher measurement sensitivity than that provided by conventional measurement models containing the MUT only.

## BIBLIOGRAPHY

- [1] J. Baker-Jarvis, R. G. Geyer, J. H. Grosvenor, M. D. Janezic, C. A. Jones, B. Riddle, C. M. Weil, and J. Krupka, "Dielectric characterization of low-loss materials a comparison of techniques," *IEEE Transactions on Dielectrics and Electrical Insulation*, Vol. 5, No. 4, pp. 571–577, 1998, doi:10.1109/94.708274.
- [2] M. W. Hyde, M. J. Havrilla, A. E. Bogle, E. J. Rothwell, and G. D. Dester, "An Improved Two-Layer Method for Nondestructively Characterizing Magnetic Sheet Materials Using a Single Rectangular Waveguide Probe," *Electromagnetics*, Vol. 32, No. 7, pp. 411–425, 2012, doi:10.1080/02726343.2012.716702.
- [3] G. D. Dester, *Electromagnetic material characterization of a conductor-backed material using the two layer, two thickness, and two iris waveguide probe methods: Error analysis, simulation, and experimental results*, 2008.
- [4] A. Possolo, and H. K. Iyer, "Invited Article: Concepts and tools for the evaluation of measurement uncertainty," *Review of Scientific Instruments*, Vol. 88, No. 1, p. 011301, 2017, doi:doi: 10.1063/1.4974274.
- [5] L. Mari, P. Carbone, and D. Petri, "Measurement Fundamentals: A Pragmatic View," *IEEE Transactions on Instrumentation and Measurement*, Vol. 61, No. 8, pp. 2107–2115, 2012, doi:10.1109/TIM.2012.2193693.
- [6] L. F. Chen, C. K. Ong, C. P. Neo, V. V. Varadan, and V. K. Varadan, *Microwave electronics: measurement and materials characterization*. John Wiley & Sons. 2004.
- [7] K. Y. You, F. B. Esa, and Z. Abbas, "Macroscopic characterization of materials using microwave measurement methods – A survey," *2017 Progress in Electromagnetics Research Symposium – Fall (PIERS – FALL)*, 2017, pp. 194–204, doi:10.1109/PIERS-FALL.2017.8293135.
- [8] S. Narang, B. Bahel, and S. Bahel, "Low loss dielectric ceramics for microwave applications: a review," *J. Ceram. Process. Res*, Vol. 11, No. 3, pp. 316–321, 2010.
- [9] J. Krupka, "Frequency domain complex permittivity measurements at microwave frequencies," *Measurement Science and Technology*, Vol. 17, No. 6, pp. R55–R70, 2006, doi:10.1088/0957-0233/17/6/r01.
- [10] J. Kui, "Microwave Dielectric Ceramic Materials and Their Industry Development Overview and Future Prospects," *Journal of Physics: Conference Series*, Vol. 1885, No. 3, p. 032034, 2021, doi:10.1088/1742-6596/1885/3/032034.
- [11] H. Howard, and D. Gilmer. *High dielectric constant materials: VLSI MOSFET applications*. Vol. 16. Springer Science & Business Media, 2006.

- [12] BIPM, IEC, et al, “Evaluation of measurement data – Guide to the expression of uncertainty in measurement,” JCGM 100:2008 (GUM 1995 with Minor Corrections), Joint Committee for Guides in Metrology, BIPM, 2008
- [13] Y. Kato, M. Horibe, M. Ameya, S. Kurokawa, and Y. Shimada. “New Uncertainty Analysis for Permittivity Measurements Using the Transmission/Reflection Method,” *IEEE Transactions on Instrumentation and Measurement*, Vol. 64, No. 6, pp. 1748–1753, 2015, doi: doi:10.1109/tim.2015.2401231.
- [14] BIPM, IEC, et al. “Evaluation of Measurement Data – Supplement 1 to the Guide to the Expression of Uncertainty in Measurement – Propagation of Distributions using a Monte Carlo Method,” BIPM, 2008.
- [15] R. Kacker, “True value and uncertainty in the GUM,” *Journal of Physics: Conference Series*, Vol. 1065, p. 212003, 2018, doi:10.1088/1742-6596/1065/21/212003.
- [16] E. Paez, M. A. Azpurua, C. Tremola, and R. Callarotti, “Uncertainty Minimization In Permittivity Measurements In Shielded Dielectric Resonators,” *Progress In Electromagnetics Research M*, Vol. 26, pp. 127–141, 2012, doi:10.2528/pierm12082811.
- [17] N. Ding, X. Cui, Y. Li, and W. Yuan, “Application of Monte Carlo Method in Uncertainty Analysis of Mismatch Factor,” *2018 Conference on Precision Electromagnetic Measurements (CPEM 2018)*, 2018, pp. 1–2, doi:10.1109/CPEM.2018.8500895.
- [18] C. Bachiller, H. Esteban, H. Mata, M. A. Valdes, V. E. Boria, A. Belenguer, and J. V. Morro, “Hybrid Mode Matching Method for the Efficient Analysis of Metal and Dielectric Rods in H Plane Rectangular Waveguide Devices,” *IEEE Transactions on Microwave Theory and Techniques*, Vol. 58, No. 12, pp. 3634–3644, 2010, doi:10.1109/TMTT.2010.2083951.
- [19] Rogers Corporation, AD1000 Laminates, see online: <https://www.rogerscorp.com/advanced-electronics-solutions/ad-series-laminates/ad1000-laminates>
- [20] Association Connecting Electronics Industries, IPC-TM-650 Test Methods Manual, see online: <https://www.ipc.org/test-methods>
- [21] DURATOOL, Digital Caliper, see online: <https://www.farnell.com/datasheets/1661929.pdf>
- [22] Exxelia Temex, Dielectric Resonators, see online: <https://exxelia.com/uploads/PDF/e7000-v1.pdf>
- [23] Arlon Microwave Materials, PTFE/Woven Fiberglass/Micro-Dispersed Ceramic Filled Laminate for RF & Microwave Printed Circuit Boards, see online: <http://www.agssales.com/ad430.pdf>

- [24] C. M. Linton, and I. Thompson, “One- and two-dimensional lattice sums for the three-dimensional Helmholtz equation,” *Journal of Computational Physics*, Vol. 228, No. 6, 2009, doi:10.1016/j.jcp.2008.11.013.
- [25] R. Kushnin, J. Semenjako and Y. V. Shestopalov, “Accelerated boundary integral method for solving the problem of scattering by multiple multilayered circular cylindrical posts in a rectangular waveguide,” *2017 Progress In Electromagnetics Research Symposium - Spring (PIERS)*, 2017, pp. 3263–3271, doi:10.1109/PIERS.2017.8262320.



**Romāns Kušņins** was born in 1986 in Riga. He obtained a Bachelor's degree in Electronics in 2009 and a Master's degree in Electronics in 2011 from Riga Technical University. He has been a lecturer and researcher at Riga Technical University since 2017. His research interests include electromagnetics, microwave devices, wireless power transfer, filter and antenna design, and applied mathematics.